University of Mohamed Khider
Biskra Faculty of Science and
Technology Department of Electrical
Engineering

MASTER THESIS

Science and Technology
Field: Electrical Engineering
Option: Electrical Machines
Ref:

Presented and submitted by:
Adissa Abdelatif

On:05 June 2025

Incorporation of Z-Source Inverter in photovoltaic system

Jury:

Mr.	Rezig Mohamed	MCA	University of Biskra	President
Ms.	Boucetta Abir	MCB	University of Biskra	Examiner
Mr.	Boussabeur Mohamed Tayeb	MCB	University of Biskra	Supervisor

Academic Year: 2024-2025

University of Mohamed Khider Biskra
Faculty of Science and Technology
Department of Electrical Engineering

MASTER THESIS

Science and Technology
Field: Electrical Engineering
Option: Electrical Machines
Ref:

Incorporation of Z-Source Inverter in photovoltaic system

On:05 June 2025

Presented By:

Adissa Abdelatif

Favorable opinion of the supervisor:

Dr. Boussabeur Mohamed Tayeb

Positive opinion of the President of the Jury

Dr.Rezig Mohamed

Stamp and signature


بسم الله الرحمن الرحيم

Abstract

This thesis studies the use of Z-source inverters (ZSI) in photovoltaic (PV) systems. Traditional inverters can only increase or decrease the voltage using extra components. In contrast, the ZSI can do both in one stage, which makes the system simpler and more efficient. The main goal of this work is to analyze how these inverters can be used in PV systems to improve performance. We model the ZSI and apply a control method (SBC Control) to manage the inverter. In addition, we use MPPT (Maximum Power Point Tracking) to maximize the power extracted from the photovoltaic panels. The system is tested through simulations using MATLAB/Simulink. The results show that the ZSI helps improve energy conversion, reduce input current ripple, and lower the stress on switching devices. This makes the system more reliable and efficient for solar energy applications.

Keywords:

Z-source inverter (ZSI), photovoltaic system, SBC Control, MPPT

Résumé

Cette thèse étudie l'utilisation d'onduleurs à source Z (ZSI) dans les systèmes photovoltaïques (PV). Les onduleurs traditionnels ne peuvent qu'augmenter ou diminuer la tension en utilisant des composants supplémentaires. En revanche, le ZSI peut faire les deux en une seule étape, ce qui rend le système plus simple et plus efficace. L'objectif principal de ce travail est d'analyser comment ces onduleurs peuvent être utilisés dans les systèmes photovoltaïques pour améliorer les performances. Nous modélisons le ZSI et appliquons une méthode de contrôle (contrôle SBC) pour gérer l'onduleur. En outre, nous utilisons le MPPT (Maximum Power Point Tracking) pour maximiser la puissance extraite des panneaux photovoltaïques. Le système est testé par des simulations utilisant MATLAB/Simulink. Les résultats montrent que le ZSI permet d'améliorer la conversion énergétique, de réduire l'ondulation du courant d'entrée et de diminuer les contraintes sur les dispositifs de commutation. Cela rend le système plus fiable et plus efficace pour les applications d'énergie solaire.

Mots-clés :

Onduleur à source Z (ZSI), système photovoltaïque, contrôle SBC, MPPT

ملخص:

تدرس هذه الأطروحة استخدام العاكسات ذات المصدر Z (ZSI) في الأنظمة الكهروضوئية (PV). يمكن للمحولات التقليدية فقط زيادة أو تقليل الجهد باستخدام مكونات إضافية. في المقابل، يمكن لمحولات ZSI القيام بالأمرين في مرحلة واحدة، مما يجعل النظام أبسط وأكثر كفاءة. الهدف الرئيسي من هذا العمل هو تحليل كيفية استخدام هذه العاكسات في الأنظمة الكهروضوئية لتحسين الأداء. نقوم بنمذجة ZSI وتطبيق طريقة تحكم (تحكم SBC) لإدارة العاكس. بالإضافة إلى ذلك، نستخدم MPPT(تتبع نقطة الطاقة القصوى) لتعظيم الطاقة المستخرجة من الألواح الكهروضوئية. يتم اختبار النظام من خلال المحاكاة باستخدام MATLAB/Simulink. تُظهر النتائج أن نظام ZSI يساعد على تحسين تحويل الطاقة وتقليل تموج تيار الإدخال وتقليل الضغط على أجهزة التحويل. وهذا يجعل النظام أكثر موثوقية وكفاءة لتطبيقات الطاقة الشمسية.

الكلمات المفتاحية:

عاكس المصدر Z (ZSI) ، النظام الكهروضوئي، التحكم فيSBC ، MPPT

Dedicates

I dedicate this work to my dear parents, may Allah protect them, who have always believed in me and supported me morally throughout my studies, Abdulkader and Houria.

My brothers: Faisal, Ismail and Mokhtar

My sisters: Fatima, Warda, Ruqaya, Saida and Hanaa

My wife and companion, Hanin, and my beautiful daughters Mayar and Ilin

My friend Islam Makhloufi

All my uncles, aunts, cousins, aunts, uncles and aunts

All my friends since childhood: Primary school (Issa Arish), middle school (Salem Bouzidi), high school (Lakhdar Ramadani)

And to all those who love me and I love them

ACKNOWLEDGMENT

ACKNOWLEDGMENT First of all, I would like to introduce my greatly indebted in my work and success to my Merciful GOD who supported me with patience and strength to complete this thesis. Cordial thanks and deep gratitude are offered to my supervisor ***Dr.Mohamed Tayeb Boussabeur*** *for the patience guidance, encouragement and supervision.*

I express my sincere gratitude to the examination committee members: ***Dr. Rezig Mohamed*** *and* ***Dr. Boucetta Abir*** *allowing my defense to be a fun experience and for their helpful criticism and recommendations. Special thanks to staff members and instructors of my department for their exerted efforts to facilitate the difficulties during the work.*

Thanks to my parents for always loving and supporting me and for giving me all I needed to do this work.

List of Figures

List of Tables

Contents

GENERAL INTRODUCTION

Photovoltaic (PV) systems have become one of the most widely used technologies for sustainable electricity generation as global demand for clean and renewable energy grows. However, PV modules produce a variable and nonlinear DC output because of changing environmental conditions such as solar irradiance and temperature. To ensure stable and efficient power delivery to the load or grid amidst this variability, effective power conditioning systems are required [1].

Conventional PV systems typically employ a two-stage power conversion architecture. This includes a DC-DC converter for maximum power point tracking (MPPT) and voltage regulation, followed by a DC-AC inverter that connects to the grid or AC loads. While functional, this approach increases complexity, costs, and energy losses, and may reduce system reliability [2]. Furthermore, traditional voltage-source inverters (VSIs) do not support voltage boosting and require complex control schemes to safely manage switching states [3].

To address these challenges, Peng proposed the Z-Source Inverter (ZSI) in 2003 as a single-stage power converter that combines DC-DC conversion and inversion functions. Its distinguishing feature is an impedance network made up of capacitors and inductors that enables a special operating mode known as "shoot-through." This state allows both switches on an inverter leg to conduct at the same time, resulting in inherent buck-boost capability within one stage and increased system robustness [4].

In PV applications, the ZSI provides several benefits, including a wider voltage operating range, improved fault tolerance, fewer power stages, and better performance under partial shading or transient conditions. These characteristics make it particularly appealing for distributed renewable energy systems requiring efficiency, cost-effectiveness, and compact design [5]. Furthermore, its shoot-through mode eliminates the need for dead-time control, which reduces electromagnetic interference and improves output waveform quality.

To fully realize the benefits of the ZSI, appropriate modulation and control strategies must be used to handle the converter's nonlinear behavior and ensure efficient MPPT. Recent research has investigated control techniques such as simple boost control, maximum boost

control, and space vector modulation, with promising results for improving system stability and performance [6].

This thesis investigates the use of Z-source inverters in photovoltaic systems, focusing on their operating principles, design considerations, and practical benefits over traditional converters. The study aims to show how ZSI technology can significantly improve the performance and dependability of PV systems.

The three chapters of this thesis are as follows:

- The first chapter explains the operating principle of the Z-source inverter, describes the various control techniques and details the modeling of this inverter.
- The second chapter is devoted to PV systems, the operating principle and PV system modeling.
- The third chapter presents our system, which proposes the integration of a z-source inverter into a DC source. The system is controlled by SBC (Simple Boost Control). Simulation was carried out using the MATLAB/Simulink environment to validate our theoretical study. Finally, a general conclusion is presented to finalize this work.

Chapter I:

Study of the Three-Phase Inverter with Z-Source Structure

1.1 Introduction

In this chapter, we explore the operation and characteristics of a specific source by analyzing its operating principles and advantages. We begin with a detailed study of the operating principle, identifying the different states of the source and the associated monitoring factor. Next, we highlight the advantages offered by this source, particularly in terms of performance and energy efficiency. We also examine its topology, emphasizing its structural specifics and practical applications. The control of the source is a crucial aspect of our analysis. We review various control strategies, such as Maximum boost control (MBC), Simple boost control (SBC), Maximum constant boost control (MCBC), and Space Vector Pulse Width Modulation (SPVWM), to compare their performance and optimal applications. Finally, we introduce the small-signal model of the Z-source, with a particular focus on the average model, which simplifies the analysis and optimization of the system's dynamic behavior.

This chapter aims to provide a comprehensive understanding of this source by combining a theoretical approach with an analysis of the most suitable control methods.

1.2 Operating Principle of Z-source inverter

The Z-source inverter not only performs the conventional function of DC-AC conversion, but it also has an additional capability similar to that of a boost converter, allowing it to increase the input voltage before converting it into alternating current [7]. This feature is made possible through a unique impedance network consisting of inductors and capacitors, which enables a controlled short-circuit state to boost the output voltage [8].

Compared to traditional voltage-source inverters (VSI) and current-source inverters (CSI), the Z-source inverter offers significant advantages, including better immunity to disturbances, reduced switching stress, and improved energy efficiency [9]. Additionally, it eliminates the need for an extra conversion stage, thus reducing system complexity and cost.

This circuit is established by grouping the switches of the three inverter legs into a single fictitious switch, denoted as D. This simplification facilitates the analysis of the overall behavior of the converter in switching mode [7]. Additionally, the three alternating current sources are replaced by a single direct current source, which reflects the energy conversion principle specific to the Z-source inverter [8]. This equivalent representation allows for the study of different control strategies and system performance under various operating conditions [9]. Furthermore, this configuration enables better management of switching states, thereby reducing switching losses and improving overall system efficiency [10].

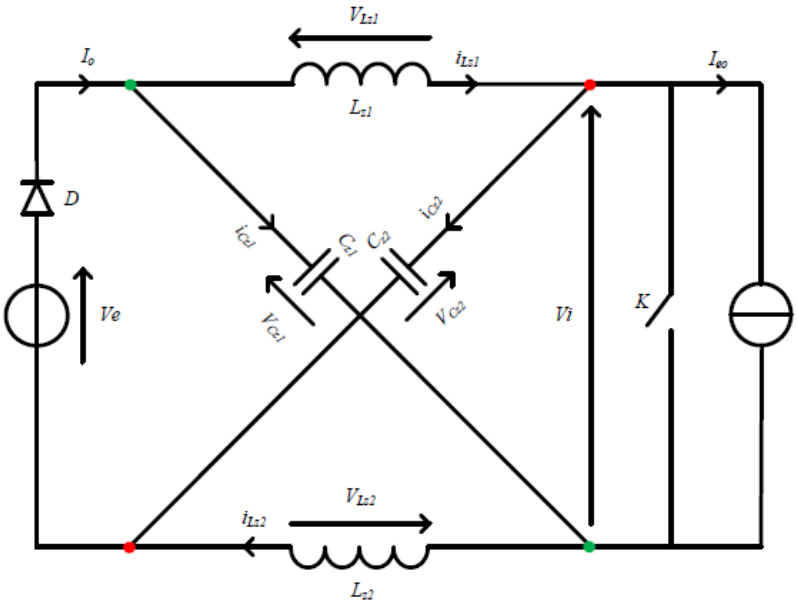

Figure 1.1 Equivalent circuit of a three-phase Z-source inverter

1.2.1 Z-Source Inverter's Shoot-Through State

During this state, both power sources, namely the voltage source and the current source, are decoupled (disconnected). This phase is essential for the operation of the Z-source inverter, as it enables a controlled short-circuit state, which is impossible in a traditional inverter. The Following phenomena can be observed:

- Blocking of the protection diode: The protection diode is reverse biased, preventing current from flowing in its natural direction. This characteristic is crucial to avoid any backflow of current to the power source and ensure efficient energy management within the Z-source network [11].
- Closure of switch K: When the fictitious switch K is closed, it establishes a conductive path that allows the reactive elements of the Z-source network to interact without directly affecting the power source [12].
- Discharge of capacitors: The capacitors discharge through the two inductors of the Z-source network. This discharge plays a key role in energy storage and transfer, as it influences the voltage across the inverter and enables the output voltage boost mode [13].
- Zero input voltage Vi: During this phase, the input voltage V_i of the converter becomes zero, reflecting the controlled short-circuit state of the Z-source inverter. Unlike conventional inverters, where a short circuit leads to failure, the Z-source inverter

utilizes this property to modulate its output voltage and enhance its voltage gain performance [14].[15]

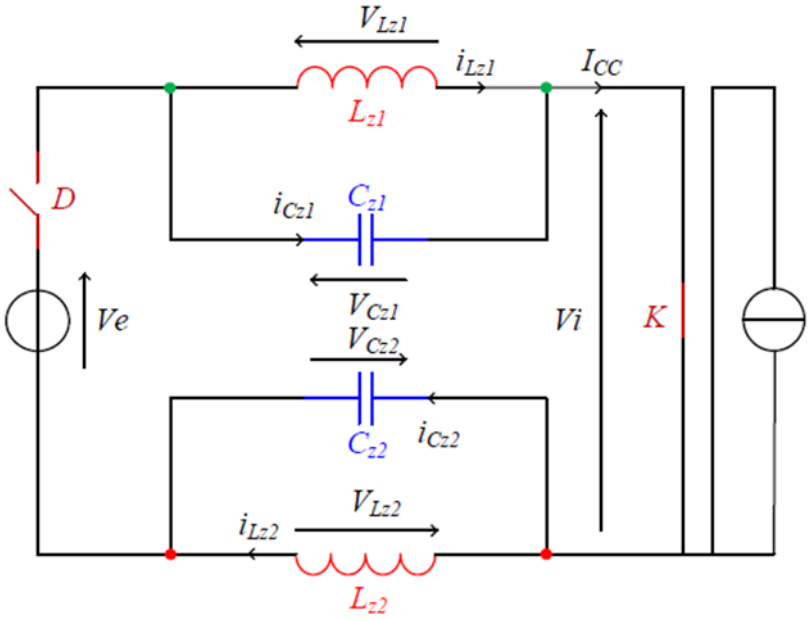

Figure 1.2 Equivalent Circuit of the Inverter Short-Circuit State

The short-circuit state can be mathematically described by the following equations:

$$\begin{cases} V_{LZ1} = V_{CZ1} \\ V_{LZ2} = V_{CZ2} \\ V_i = 0 \end{cases} \begin{cases} i_{CZ1} = -i_{LZ1} \\ i_{CZ2} = -i_{LZ1} \end{cases} \quad (1.1)$$

1.2.2 Active States in a Z-Source Inverter

The active states in the operation of a Z-source inverter correspond to the phases during which energy is efficiently transferred between the power source and the load. Unlike the shoot-through state, where the sources are decoupled, here, both sources are coupled, allowing a smooth energy transfer through the main converter circuit and the impedance network. This process plays a key role in power conversion and enables the inverter to offer enhanced performance compared to conventional structures. During these states, the following phenomena can be observed:

- Conducting protection diode: The diode is forward biased, allowing current to flow. It plays a crucial role in ensuring energy flow continuity and protecting the circuit

- Maximum voltage at the converter input: The voltage V_i reaches its peak value, enabling the output voltage to exceed the input voltage, unlike conventional inverters. This capability is one of the main advantages of the Z-source inverter over other architectures [16].
- Blocking of switch K: The fictitious switch K, modeling the global switching state of the circuit, is open, preventing current from flowing through the inverter legs and avoiding any internal short circuit.
- Discharge of inductors: The energy stored in the inductors is released into the converter circuit. This step contributes to stabilizing the output voltage and improving the system's energy efficiency [17].

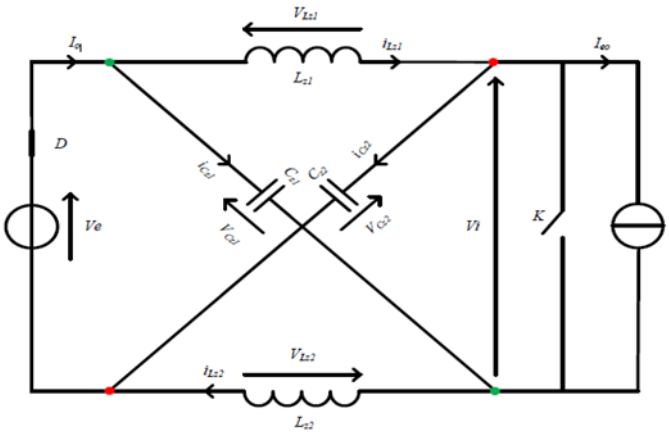

Figure 1.3 Equivalent Circuit of the Inverter's Active States

The short-circuit state can be mathematically described by the following equations:

$$\begin{cases} V_{LZ1} = V_e - V_{CZ2} \\ V_{LZ2} = V_e - V_{CZ1} \\ V_i = V_{CZ1} - V_{LZ1} \\ V_i = V_{CZ2} - V_{LZ2} \end{cases} \begin{cases} i_{CZ1} = i_{LZ1} - I_{eo} \\ i_{CZ2} = i_{LZ1} - I_{eo} \end{cases} \quad (1.2)$$

1.2.3 Monitoring Factor B

The boost factor is a key parameter that defines the operation of a Z-source inverter. It determines the converter's ability to step up the input voltage and is defined as the ratio between the peak value of the voltage Vi at the input of the main circuit (composed of the three inverter legs) and the input voltage V_e.

This factor is essential for applications requiring voltage boosting without the need for an additional DC-DC converter. Unlike conventional inverters, the Z-source inverter enables more efficient voltage conversion, making it particularly suitable for photovoltaic systems, electric vehicles, and motor drives [16].[Mohamed T. Boussabeur1,15]

$$\begin{cases} V_{LZ1} = V_{LZ2} - V_{LZ} \\ V_{CZ1} = V_{CZ2} - V_{CZ} \end{cases} \begin{cases} i_{LZ1} = i_{LZ2} = i_{LZ} \\ i_{CZ1} = i_{CZ2} = i_{LZ} \end{cases} \quad (1.3)$$

Using equations, I-1 and I-3, we find that:

$$\begin{cases} V_{LZ} = V_{CZ} \\ V_{CZ1} = 0 \end{cases} \begin{cases} V_{LZ} = V_e - V_{CZ} \\ V_i = V_e - V_{LZ} \end{cases} \quad (1.4)$$

Suppose that the duration of the short-circuit state (shoot-through) is T_{CC}, and T represents the period of a switching cycle. The average value of the inductor voltage la V_{Lz} over this cycle must be zero, and it is given by the following equation:

$$(V_{LZ}) = \frac{T_{cc}V_c + (T - T_{cc})(V_e - V_{cz})}{T} = 0 \quad (1.5)$$

From this relation, we can deduce the expression for the capacitor voltage V_{CV} as follows:

$$V_{cz} = \frac{(T - T_{cc})}{(T - 2T_{cc})} V_e \quad (1.6)$$

Equations 1.4 allow us to write the expression for the peak value of the voltage V_i:

$$\hat{V}_i = 2V_{CZ} - V_e \quad (1.7)$$

Replacing V_{cz} with its expression from equation 1.6, we obtain the following relation:

$$\hat{V}_i = \frac{T}{(T - 2T_{cc})} V_e \quad (1.8)$$

This voltage can also be expressed using the duty cycle d of the short-circuit state, by the following relation:

$$\hat{V}_i = \frac{1}{(1 - 2d)} V_e = B.V_e \quad (1.9)$$

With

$$d = \frac{T_{cc}}{T} \tag{1.10}$$

And

$$B = \frac{1}{(1-2d)} \tag{1.11}$$

This result represents the well-known boost ratio of the Z-source inverter, where the duty cycle evolves within the interval [0, 0.5]. It has been established by neglecting losses in the switches (diodes and IGBTs of the inverter) as well as resistive voltage drops.

This factor is used along with the amplitude ratio r (regulation coefficient) to define the total gain of the converter G as follows:

$$G = \frac{V_{out\,max}}{V_e} = B.r = \frac{r}{1-2d} \quad et \;\; r = \frac{V_{out\,max}}{V_{i/2}} \tag{1.12}$$

The expression of this gain shows that the Z-source inverter can operate in both boost and buck modes in the same direction. This operating mode provides the ability to deliver AC output voltages that are independent of the DC input voltage, unlike conventional voltage inverters, where the DC voltage must be higher than the desired AC voltage.

1.3 Advantages of a Source

1.3.1 Single-Stage Conversion for Buck Boost Operation

Z-source converters enable simultaneous buck (step-down) and boost (step-up) operations in a single stage. This capability eliminates the need for an additional DC-DC converter, thereby simplifying the system design, reducing energy losses, and improving overall efficiency.

- Impact on Efficiency: Integrating the buck-boost function in one stage reduces losses associated with multiple conversion stages, which is particularly beneficial in applications such as photovoltaic systems and electric vehicles.
- Application Example: In a grid-connected PV system, a traditional converter requires a boost converter to raise the solar panel voltage before converting it to AC. A Z-source inverter performs this function in a single stage, reducing both complexity and cost.[16]

1.3.2 Increased Flexibility in Energy Source Integration

The Z-source converter can operate with both voltage sources and current sources, making it particularly versatile. It easily adapts to a variety of energy sources, including:

- Renewable Sources: Suited for the voltage fluctuations found in photovoltaic and wind systems.
- Energy Storage Systems: Compatible with batteries and fuel cells that have variable output voltages.
- Hybrid Systems: Allows simultaneous integration of multiple types of energy sources [18].

1.3.3 Enhanced Reliability and Fault Tolerance

Z-source converters effectively address issues related to short circuits and electromagnetic interference (EMI):

- Controlled Shoot-Through Capability: Instead of completely avoiding shoot-through, the Z-source topology incorporates controlled shoot-through states, thereby enhancing fault tolerance.
- EMI Protection: The design of the impedance network offers better immunity to electromagnetic disturbances, reducing the risk of misfiring due to switching errors.[17]

1.3.4 Reduced Component Count and Lower Costs

By eliminating the need for a separate DC-DC conversion stage, Z-source converters require fewer components, which results in:

- Reduced Material Costs: Fewer inductors, capacitors, and switching devices are needed.
- Compact Design: With fewer components, the overall system size is reduced, making Z-source converters ideal for applications with limited space (such as electric vehicles and aerospace systems) [19].

1.3.5 Improved Power Quality and Harmonic Reduction

The absence of dead time (thanks to the controlled use of shoot-through states) leads to:

- Higher Output Voltage Quality: Reduced total harmonic distortion (THD) lessens stress on connected loads and improves energy efficiency.
- Optimized Motor Drive Performance: Drive systems benefit from faster torque response and reduced thermal losses due to a cleaner output waveform.[20]

1.4 Topology of Z-Source

The three-phase voltage-source inverter with a Z-source structure consists of several key components that enable efficient and flexible power conversion. Unlike conventional voltage-source inverters, this topology allows both step-up and step-down voltage conversion without requiring an additional DC-DC conversion stage [21], [22]. It primarily consists of:

- A main circuit, which includes the three switching cells (inverter legs). Each cell consists of two electronic switches (IGBTs or MOSFETs) operating in a complementary manner. These cells are controlled to generate three-phase AC voltages adapted to connected loads [21].
- A Z-source impedance network, which plays a crucial role in the inverter's operation. It consists of two inductors and two capacitors arranged in an X-shape. This impedance network enables the inverter to operate in both boost and buck modes, providing a significant advantage over conventional inverters in terms of voltage regulation flexibility.
- A protection diode, placed between the DC voltage source and the impedance network. Its primary function is to prevent the discharge of the impedance network capacitors into the DC power source, ensuring better isolation and reducing the risk of overvoltage.

With this configuration, the Z-source inverter can generate an AC voltage whose amplitude can be adjusted independently of the DC input voltage. This operational flexibility makes it highly suitable for applications requiring efficient energy conversion, such as photovoltaic systems and electric motor drives [21],[22].

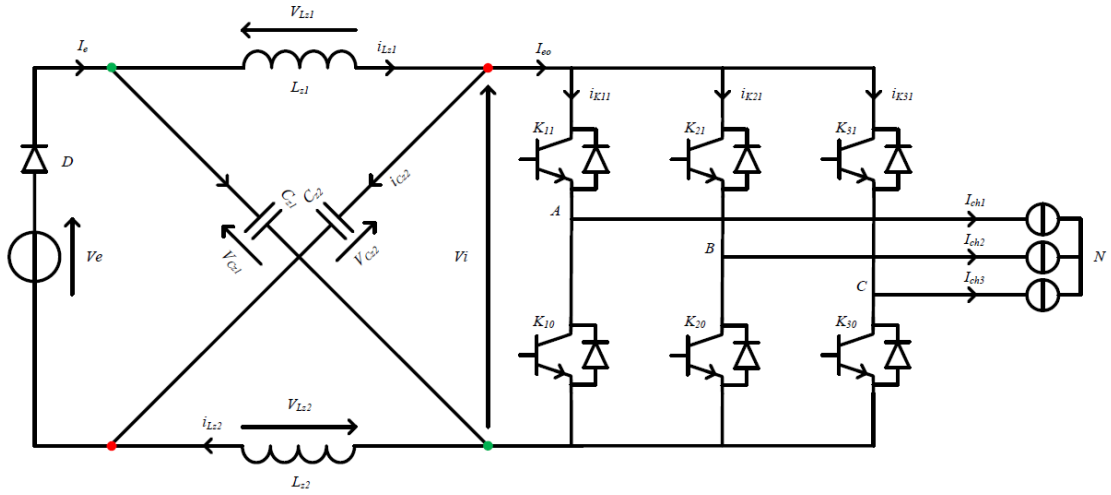

Figure 1.4 Topology of a Three-Phase Z-Source Inverter

Each leg (switching cell) consists of two bidirectional switches operating in a complementary manner to facilitate energy transfer between the two sources [11], [12].

The integration of the impedance network enables the simultaneous conduction of both switches within the same leg, a condition strictly forbidden in conventional voltage inverters. This leads to a unique operational state known as the "shoot-through state" [11], [13].

This state can only be introduced during the zero state of the converter. The impedance network functions as both an energy source and a filter. The inductors help in limiting current ripples during the shoot-through state, while the capacitors absorb these ripples and maintain a stable voltage. This design ensures the delivery of a regulated sinusoidal output voltage [12], [13].

1.5 Z-Source Control

The control of Z-source inverters plays a crucial role in optimizing their performance, particularly in improving efficiency, reducing harmonic distortions, and effectively managing the voltage boost factor [10],[11]. Unlike conventional voltage-source inverters, Z-source inverters offer a more flexible power conversion by integrating both boost and buck operation modes within the same system [12].

Several control strategies have been developed to fully exploit the benefits of this architecture. Among these techniques, we distinguish:

1.5.1 Maximum boost control (MBC) :

With the MBC method, the entire zero-state time period is transformed into the shoot-through state, leading to improved performance compared to the SBC approach. In this strategy,

the circuit enters the shoot-through state whenever the triangular carrier waveform exceeds the highest reference value (V_a, V_b, V_c) or falls below the lowest reference value.

As a result, the shoot-through duty cycle varies with each cycle. The corresponding equations can be expressed as follows:

$$\begin{cases} d_0 = \frac{2\pi - 3\sqrt{3}M}{2\pi} \\ B = 3\sqrt{3}G - 1 = \frac{\pi}{3\sqrt{3}M - \pi} \\ G = \frac{\pi M}{3\sqrt{3}M - \pi} \\ V_{dc} = BV_g = \frac{3\sqrt{3}G - \pi}{\pi} V_g \end{cases} \tag{1.13}$$

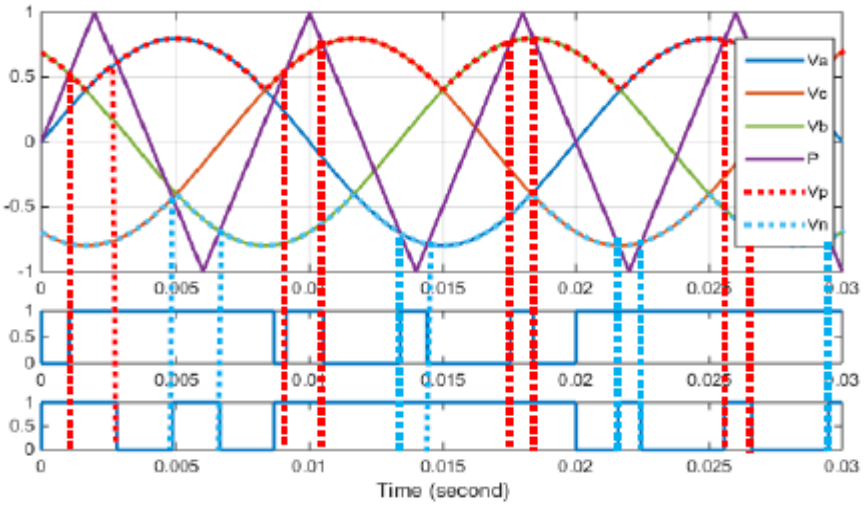

Figure 1.5 The MBC strategy reference signals

1.5.2 Simple boost control (SBC)

In addition to the conventional sinusoidal PWM technique, the simple boost control method introduces two reference lines, positioned at the peak value of the three-phase signals, to regulate the shoot-through duty cycle. When the triangular carrier waveform surpasses the upper reference threshold V_p or drops below the lower reference threshold V_n the circuit transitions into the shoot-through state. Otherwise, it follows the standard carrier-based PWM operation.

In this approach, the voltage gain of the Z-source inverter is given by:

$$G = \frac{M}{2M - 1} \tag{1.14}$$

Additional relevant equations are derived accordingly.

$$\begin{cases} d_0 = 1 - M \\ B = 2G - 1 = \frac{1}{2M-1} \\ V_{dc} = BV_g = (2G-1)V_g \end{cases} \quad (1.15)$$

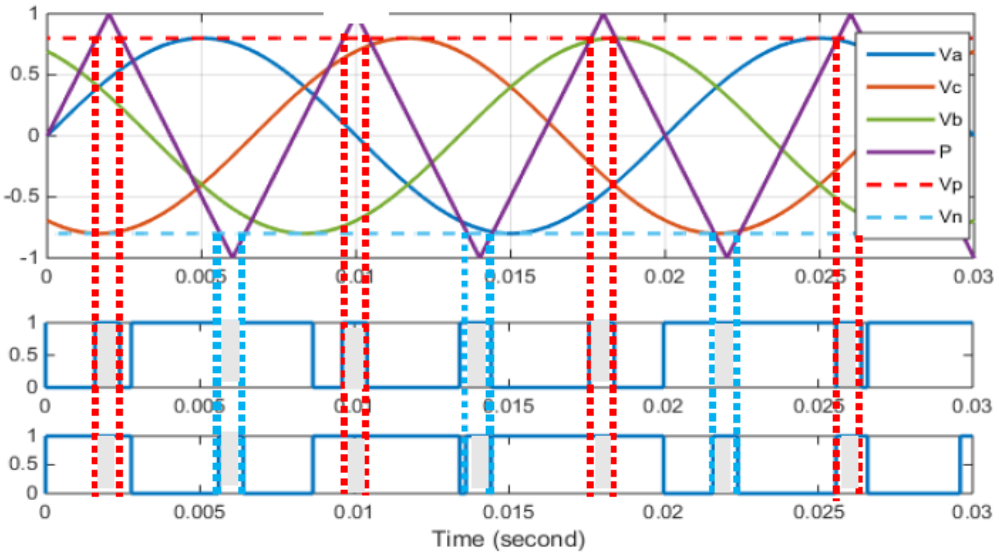

Figure 1.6 The SBC strategy reference signals

1.5.3 Maximum constant boost control (MCBC)

To optimize both volume and cost, it is crucial to maintain a constant shoot-through duty ratio. Keeping this ratio stable ensures efficient operation while minimizing component size and expense. Additionally, achieving a higher voltage boost for a given modulation index is beneficial, as it helps reduce voltage stress across the switching devices, thereby enhancing system reliability and efficiency.

The maximum constant boost control method is specifically designed to maximize voltage gain while maintaining a fixed shoot-through duty ratio. This approach enhances performance by preventing excessive variations in the shoot-through period, which could otherwise impact stability and efficiency.

A key feature of this method is the injection of a third harmonic into the modulation signal. This technique involves adding a sinusoidal signal whose frequency is precisely three times that of the fundamental reference wave. Typically, the amplitude of the injected third harmonic is set at approximately one-sixth of the modulating wave's amplitude. By incorporating this harmonic component, the control strategy improves voltage utilization, reduces total harmonic distortion (THD), and enhances the overall performance of the inverter.

The separation between these two curves plays a crucial role in defining the shoot-through duty ratio. This distance remains constant for a specific modulation index and is mathematically expressed as $\sqrt{3}$ M. Maintaining a fixed shoot-through ratio is essential for ensuring stable operation and achieving a consistent voltage boost.

By keeping this ratio unchanged, the inverter can effectively regulate the output voltage while minimizing stress on the power switches. This approach enhances overall efficiency and reduces switching losses, making the system more reliable. [23].

As a result, the corresponding mathematical expressions governing the relationship between the shoot-through ratio, modulation index, and voltage gain can be derived as follows:

$$\begin{cases} d_0 = 1 - \frac{\sqrt{3}}{2}M \\ B = 3\sqrt{3}G - 1 = \frac{1}{\sqrt{3}M-1} \\ G = \frac{M}{\sqrt{3}M-1} \\ V_{dc} = BV_g = (\sqrt{3}G - 1)V_g \end{cases} \quad (1.16)$$

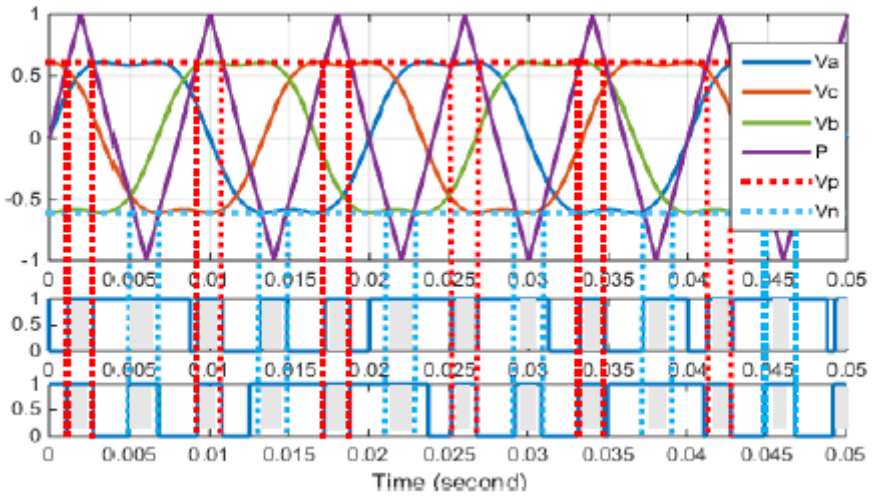

Figure 1.7 The MCBC strategy reference signals

1.5.4 Space Vector Pulse Width Modulation (SVPWM)

To implement this concept in a Z-source inverter, a modified Space Vector Pulse Width Modulation (SVPWM) technique is required. This modification allows the introduction of shoot-through states within the zero vectors while preserving the active states, ensuring efficient power conversion.

In conventional SVPWM, switching states are carefully selected to optimize the inverter's output voltage and reduce harmonic distortion. However, in a Z-source inverter, additional

control is necessary to incorporate the shoot-through states without affecting the fundamental modulation strategy. By embedding the shoot-through states within the zero vectors, the inverter can achieve voltage boosting capabilities while maintaining smooth and stable operation.

This modified SVPWM technique enhances the inverter's ability to regulate voltage gain and improves its overall performance. The approach ensures that the shoot-through period does not interfere with active switching states, thereby minimizing power losses and stress on switching components.

The switching states for a standard SVPWM implementation have been previously analyzed and are well-documented in the literature [10].

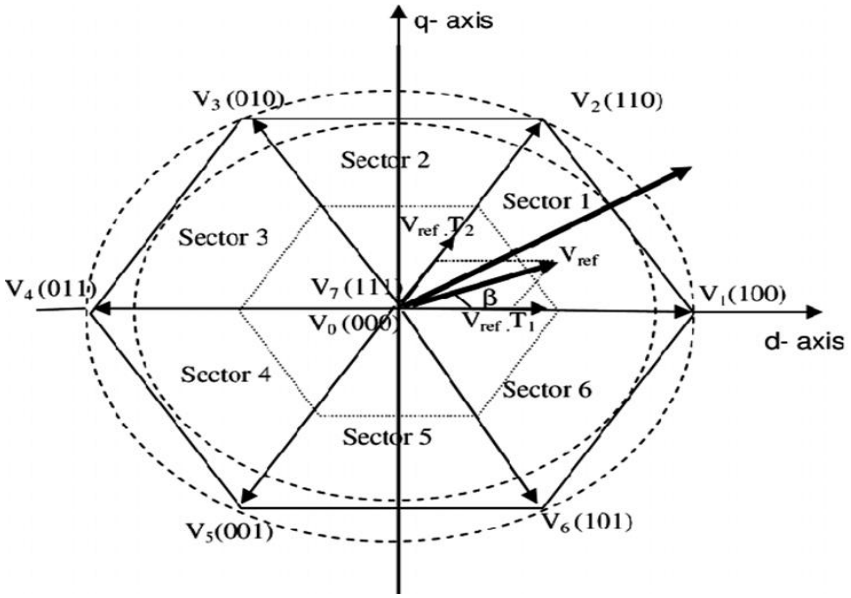

Figure 1.8 Conventionnel SVPWM

The shoot-through states are strategically distributed evenly within each switching period to ensure balanced operation and optimal performance of the Z-source inverter. This even distribution is crucial as it prevents any negative impact on the active vectors in the SVPWM algorithm while effectively introducing the shoot-through states into the system [23].

By carefully embedding the shoot-through states within the zero vectors, the inverter maintains its desired output characteristics without distorting the fundamental voltage waveform. This method enhances voltage gain while keeping the switching stress on power devices at a manageable level. The proper placement of shoot-through periods within the zero vectors also contributes to reducing electromagnetic interference (EMI) and improving the overall efficiency of the inverter.

Moreover, this approach ensures that the voltage boost capability of the Z-source network is fully utilized without interfering with the fundamental modulation process. By maintaining a consistent shoot-through duty cycle, the inverter achieves a stable operation, minimizing losses and maximizing power conversion efficiency. Proper shoot-through distribution also helps in achieving better control over the output waveform, improving the overall dynamic response of the system.

1.6 Modeling of Z-source

Designing effective regulators for the ZSC requires rigorous modeling and thorough analysis of the system's dynamic behavior. A well-defined small-signal model proves indispensable, as it delivers both a holistic and granular perspective of the system's operational characteristics. Such a model not only facilitates the optimal sizing of passive components but also enhances the identification of the system's performance boundaries and constraints [21].

There are multiple modeling techniques for electrical converters. Although the form of the result differs across these methods, they all yield the same model when components are assumed to be ideal. The following assumptions are considered:

- The ZSC operates in continuous conduction mode (CCM).
- The passive components (capacitors and inductors) of the ZS network, diode S1, and IGBT S2 are assumed to be ideal.
- The input voltage is considered independent (constant/steady).

1.6.1 The Average Model

The state-space description of a system is a canonical form of writing the differential equations that govern the system. For a linear system, the derivatives of the state variables are expressed as linear combinations of the system's inputs and the state variables themselves.

In general, energy storage elements are considered when selecting state variables; in other words, the voltages across capacitors and currents through inductors are chosen. At each instant, the state variables depend on the system's previous state. If the system's state (initial values) is known at a time t0*t*0, and if the system's inputs for t>t0*t*>*t*0 are known, then the system's equations can be solved to determine its state at any future time [22].

The state equations of the system can be expressed in the following compact form:

$$K\frac{dx(t)}{dt} = Ax(t) + Bu(t) \tag{1.17}$$

$$y(t) = \quad Cx(t) \quad + \quad Eu(t) \tag{1.18}$$

x(t) : vector containing the state variables

u(t) : vector of the system's independent inputs

K: matrices containing the values of capacitances and inductances.

A et B: matrices containing proportionality constants

If we want to compute other linear combinations of the state variables that do not coincide with the state variables or the system inputs, they are combined into a vector $y(t)$ called the output vector, where C and E are proportionality matrices. Let us consider the following variables as state variables:

$$x(t) = [i_{L1}(t)\ i_{L2}(t)\ v_{c1}(t)\ v_{c2}(t)\ i_l(t)] \tag{1.19}$$

Equations allow us to write the state-space model of the system in the form

For t ∈ $[0, DT]$

$$\begin{pmatrix} L_1 & 0 & 0 & 0 & 0 \\ 0 & L_2 & 0 & 0 & 0 \\ 0 & 0 & C_1 & 0 & 0 \\ 0 & 0 & 0 & C_2 & 0 \\ 0 & 0 & 0 & 0 & L_l \end{pmatrix} \frac{d}{dt} \begin{pmatrix} i_{L1(t)} \\ i_{L2(t)} \\ v_{c1(t)} \\ v_{c2(t)} \\ i_{l(t)} \end{pmatrix} = \begin{pmatrix} 0 & 0 & 1 & 0 & 0 \\ 0 & 0 & 0 & 1 & 0 \\ -1 & 0 & 0 & 0 & 0 \\ 0 & -1 & 0 & 0 & 0 \\ 0 & 0 & 0 & 0 & -R_l \end{pmatrix} \begin{pmatrix} i_{L1(t)} \\ i_{L2(t)} \\ v_{c1(t)} \\ v_{c2(t)} \\ i_{l(t)} \end{pmatrix} \tag{1.20}$$

Such as

$$A_1 = \begin{pmatrix} 0 & 0 & 1 & 0 & 0 \\ 0 & 0 & 0 & 1 & 0 \\ -1 & 0 & 0 & 0 & 0 \\ 0 & -1 & 0 & 0 & 0 \\ 0 & 0 & 0 & 0 & -R_l \end{pmatrix}; B_1 = \begin{pmatrix} 0 \\ 0 \\ 0 \\ 0 \\ 0 \end{pmatrix}; K = \begin{pmatrix} L_1 & 0 & 0 & 0 & 0 \\ 0 & L_2 & 0 & 0 & 0 \\ 0 & 0 & C_1 & 0 & 0 \\ 0 & 0 & 0 & C_2 & 0 \\ 0 & 0 & 0 & 0 & L_l \end{pmatrix} \tag{1.21}$$

for t ∈ [DT, T]:

$$\begin{pmatrix} L_1 & 0 & 0 & 0 & 0 \\ 0 & L_2 & 0 & 0 & 0 \\ 0 & 0 & C_1 & 0 & 0 \\ 0 & 0 & 0 & C_2 & 0 \\ 0 & 0 & 0 & 0 & L_l \end{pmatrix} \frac{d}{dt} \begin{pmatrix} i_{L1(t)} \\ i_{L2(t)} \\ v_{c1(t)} \\ v_{c2(t)} \\ i_{l(t)} \end{pmatrix} = \begin{pmatrix} 0 & 0 & 1 & 0 & 0 \\ 0 & 0 & 0 & 1 & 0 \\ -1 & 0 & 0 & 0 & 0 \\ 0 & -1 & 0 & 0 & 0 \\ 0 & 0 & 0 & 0 & -R_l \end{pmatrix} \begin{pmatrix} i_{L1(t)} \\ i_{L2(t)} \\ v_{c1(t)} \\ v_{c2(t)} \\ i_{l(t)} \end{pmatrix} + \begin{pmatrix} 1 \\ 1 \\ 1 \\ 1 \\ 1 \end{pmatrix} V_g(t) \tag{1.22}$$

Such as

$$A_2 = \begin{pmatrix} 0 & 0 & 0 & -1 & 0 \\ 0 & 0 & -1 & 0 & 0 \\ 0 & 1 & 0 & 0 & -1 \\ 1 & 0 & 0 & 0 & -1 \\ 0 & 0 & 1 & 1 & -R_l \end{pmatrix}, B_2 = \begin{pmatrix} 1 \\ 1 \\ 0 \\ 0 \\ -1 \end{pmatrix} \quad (1.23)$$

As part of converter modeling, it is essential to consider state representation. This approach ensures model stability averaged over the switching period. This implies that the natural frequency of the system must be lower than the switching frequency to guarantee model consistency. Mean state space is a fundamental concept in electrical engineering. It is defined as the mean of discrete-time random variables. In applied mathematics, the mean state space is used to solve equilibrium equations, which in turn allow us to deduce the small-signal model. This model, also known as the Small Signal Model, is an essential tool for understanding electrical systems.

The mean-state model, on the other hand, is a representation of the converter at equilibrium. It is expressed as follows:

$$0 = AX + BU \quad (1.24)$$

$$Y = CX + EU \quad (1.25)$$

The equilibrium matrices are as follows:

$$A = DA_1 - \overline{D}A_2 \quad (1.26)$$

$$B = DB_1 - \overline{D}B_2 \quad (1.27)$$

$$C = DC_1 - \overline{D}C_2 \quad (1.28)$$

$$E = DE_1 - \overline{D}E_2 \quad (1.29)$$

Such as:

X=Equilibrium state vector

U=Equilibrium input vector

Y=Equilibrium output vector

D=Equilibrium duty cycle

$$D = 1 - \overline{D} \quad (1.30)$$

The equations of state for the small-signal model are:

$$K\frac{d\hat{x}(t)}{dt} = A\hat{x}(t) + B\hat{u}(t) + \{(A_1\_A_2)X + (B_1\_B_2)U\}\hat{d}(t) \quad (1.31)$$

After Laplace transformation, we find:

$$sL_1\hat{\imath}_{L1}(s) = D\hat{v}_{c1}(s) - \bar{D}\hat{v}_{c2}(s) + \bar{D}\hat{v}_g(s) + (V_{C1} + V_{C2} - Vg)\hat{d}(s) \quad (1.32)$$

$$sL_2\hat{\imath}_{L2}(s) = \bar{D}\hat{v}_{c1}(s) + D\hat{v}_{c2}(s) + \bar{D}\hat{v}_g(s) + (V_{C1} + V_{C2} - Vg)\hat{d}(s) \quad (1.33)$$

$$sC_1\hat{v}_{C1}(s) = -D\hat{\imath}_{L1}(s) + \bar{D}\hat{\imath}_{L2}(s) - \bar{D}\hat{\imath}_l(s) + (-I_{L1} - I_{L2} + I_l)\hat{d}(s) \quad (1.34)$$

$$sC_2\hat{v}_{C2}(s) = -D\hat{\imath}_{L2}(s) + \bar{D}\hat{\imath}_{L1}(s) - \bar{D}\hat{\imath}_l(s) + (-I_{L1} - I_{L2} + I_l)\hat{d}(s) \quad (1.35)$$

$$sL_l\hat{\imath}_l(s) = \bar{D}\hat{v}_{c1}(s) + \bar{D}\hat{v}_{c2}(s) - \bar{D}\hat{v}_g(s) + (-V_{C1} - V_{C2} + Vg)\hat{d}(s) - R_l\hat{\imath}_l(s) \quad (1.36)$$

According to the previous assumption (L1=L2=L et C1=C2=C), we have a symmetrical impedance network, and combining (2.7) and (2.8) we obtain:

$$\hat{\imath}_{L1}(t) - \hat{\imath}_{L2}(t) = \frac{1}{sL}[\hat{v}_{C1}(t) - \hat{v}_{C2}(t)] \quad (1.37)$$

Similarly, for (2.9) and (2.10):

$$sC[\hat{v}_{C1}(t) - \hat{v}_{C2}(t)] = -\frac{1}{sL}[\hat{v}_{C1}(t) - \hat{v}_{C2}(t)] \quad (1.38)$$

Hence

$$(1 + s^2LC)[\hat{v}_{C1}(t) - \hat{v}_{C2}(t)] = 0 \quad (1.39)$$

This equation allows us to conclude that at each frequency different from the resonance frequency, i.e. $\omega \neq \sqrt{\frac{1}{LC}}$, we have:

$$\hat{v}_{C1}(t) = \hat{v}_{C2}(t) = \hat{v}_C(t) \text{ and } \hat{\imath}_{L1}(t) = \hat{\imath}_{L2}(t) = \hat{\imath}_L \quad (1.40)$$

So, the equations and matrices above can be simplified. Returning to (2.5), we can derive the equilibrium equations for the converter:

$$\begin{pmatrix}0\\0\\0\end{pmatrix} = \begin{pmatrix}0 & D-\bar{D} & 0\\ D-\bar{D} & 0 & -\bar{D}\\ 0 & 0 & -R_l\end{pmatrix}\begin{pmatrix}I_L\\V_C\\I_l\end{pmatrix} + \begin{pmatrix}\bar{D}\\0\\-\bar{D}\end{pmatrix}V_g \quad (1.41)$$

Solving these algebraic equations gives the values of the equilibrium state variables:

$$V_C = \frac{\bar{D}}{\bar{D}-D} V_g \tag{1.42}$$

$$I_L = \frac{\bar{D}}{\bar{D}-D} I_l \tag{1.43}$$

$$I_l = \frac{V_C}{R_l} \tag{1.44}$$

1.6.2 Small signal model

In order to determine the dynamic behavior of the state variables, the input voltage and duty cycle of the Shoot-Through will be perturbed around their equilibrium values, and can be written as:

$$vg(t) = Vg + vg(t) etd(t) = D + d(t) \tag{1.45}$$

Such as:

Vg and D: equilibrium values.

$\widehat{v_g}$and $\hat{d}$(t): disturbance values.

The resulting disturbances of the state variables can be written as:

$$x(t) = X + \hat{x}(t) \tag{1.46}$$

where: x(t) represents the vector of state variables reduced according to (2.12) a

$$x(t) = [i_L(t)\ \ v_c(t)\ i_l(t)] \tag{1.47}$$

The state equations of the small-signal model, found using equation (2.6) after application of the Laplace transformation, these transfer functions can also be reduced to:

$$sL\hat{\imath}_L(s) = (D - \bar{D})\hat{v}_c(s) + \bar{D}\hat{v}_g(s) + (2V_c - V_g)\hat{d}(s) \tag{1.48}$$

$$sC\hat{v}_C(s) = (\bar{D} - D)\hat{\imath}_L(s) - \bar{D}\hat{\imath}_l(s) + (2I_L - I_l)\hat{d}(s) \tag{1.49}$$

$$sL_l\hat{\imath}_l(s) = 2\bar{D}\hat{v}_c\,(s) - \bar{D}\hat{v}_c + (-2V_c + V_g)\hat{d}(s) - R_l\,\hat{\imath}_l\,(s) \tag{1.50}$$

Three equivalent circuits are shown in figure (2.5) (Small signal circuits) based on the three equations (4.15). Each circuit has independent sources and sources dependent on other ZSC voltages and currents.

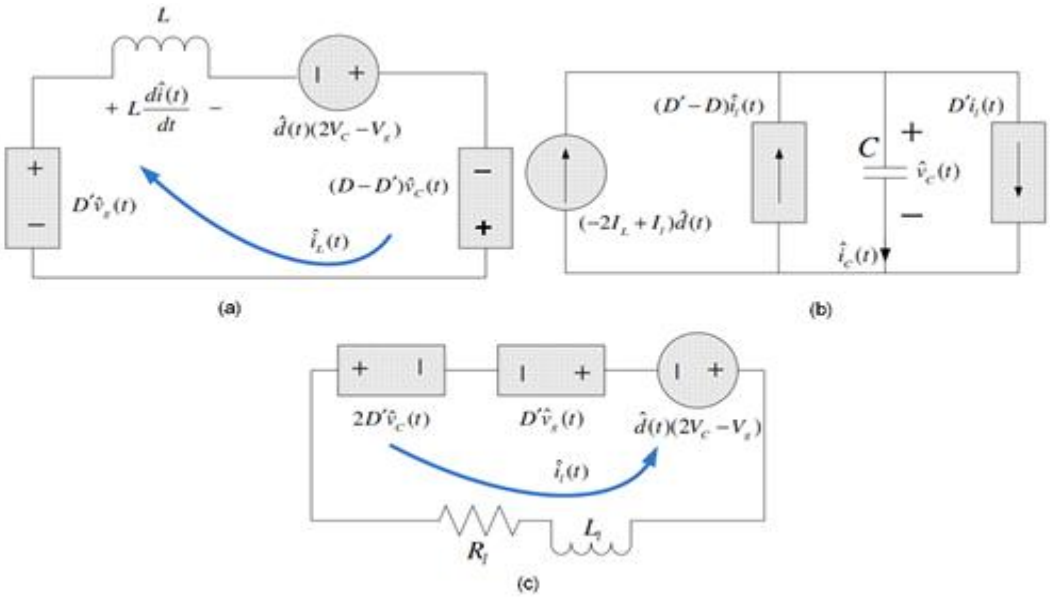

Figure 1.9: equivalent circuit (small-signal model)

At the start of the analysis, two sources of disturbance were considered, the voltage vg(t) and the Shoot-Through duty cycle d(t). It is known that the disturbance of a state variable can be expressed as a linear combination of all disturbance sources [24], hence the expression for the voltage across the capacitor:

$$\hat{v}_C(s) = G_{vg}(s)\hat{v}_g(s) + G_{vd}(s)\hat{d}(s) \tag{1.51}$$

And the expression for the inductance current is:

$$\hat{\imath}_L(s) = G_{ig}(s)\hat{v}_g(s) + G_{id}(s)\hat{d}(s) \tag{1.52}$$

Where:

$G_{vg}(s)$ is the transfer function linking the input voltage to the voltage across the capacitor.

$G_{vd}(s)$ is the transfer function between $\hat{v}_C$ and the cyclic ratio $\hat{d}$.

$G_{ig}(s)$ and $G_{id}(s)$ are the transfer functions between inductor current and input voltage and duty cycle, respectively.

1.7 Conclusion

The Z-source inverter is a new and important idea in power conversion. It solves the problems found in traditional voltage-source and current-source inverters. In this chapter, we introduced the Z-source inverter, which can both increase and decrease voltage using only one stage. This makes it a simple, flexible, and efficient solution for many powers applications.

Chapter II:

General Study of the photovoltaic system

2 Chapter II: General Study of the photovoltaic system

2.1 Introduction

The photovoltaic (PV) system is regarded as a leading technology for the harnessing of renewable energy, specifically solar power. The utilization of solar cells enables the direct transformation of sunlight into electricity, thereby eliminating reliance on combustion processes and the subsequent release of harmful emissions. The chapter commences with an examination of the configuration and foundational tenets of photovoltaic systems. In the following section, the focus shifts to the exploration of strategies that have been identified as effective in the optimization and control of performance. The discussion concludes with the development of accurate models to simulate PV system behavior under varying conditions.

2.2 Historical overview:

Humanity has always known the power of the sun and it is interesting to observe how the use of energy from the sun has evolved. In reality this energy such as the use of light or the sun is much older. Thousands of years ago, different civilizations honored the sun as a true god. In 212 BC, Archimedes used the sun to stop the Roman fleet using polished bronze mirrors. With these mirrors he succeeded in setting fire to the fleet from a distance. Several decades separated the first specific photovoltaic applications from the technological maturity allowing wide access to electricity [25].

Key Dates in Photovoltaic History [26]**:**

- 1839: The transformation of sunlight into electric current goes back to this date, the French physicist Edmond Becquerel discovered the process of using sunlight to produce electric current in a solid material. This is the photovoltaic effect
- 1875: Werner Von Siemens exhibited before the Berlin Academy of Sciences an article on the photovoltaic effect in semiconductors. But until the Second World War, the phenomenon was still a laboratory curiosity.
- 1905: Albert Einstein wrote that light could enter the interior of atoms and that the collision between photons and atoms could knock electrons out of their orbits and allow the creation of an electric current.
- 1912: Albert Einstein will be the first to explain the photovoltaic effect phenomenon, and receives the Nobel Prize in Physics in 1921 for this explanation.

- 1954: Three American researchers, Chapin, Pearson and Prince, developed a high efficiency photovoltaic cell at a time when the emerging space industry was looking for new solutions to power its satellites
- 1958: A cell with an efficiency of 9% is developed. The first satellites powered by solar cells are sent into space.
- 1973: The first house powered by photovoltaic cells is built at the University of Delaware.
- 1983: The first solar-powered car, running on photovoltaic energy, traveled 4,000 km in Australia.
- 1995: Grid-connected photovoltaic roof programs were launched in Japan and Germany, becoming widespread after 2001

2.3 Photovoltaic System

A photovoltaic (PV) system is a technology designed to convert sunlight directly into electrical energy using the photovoltaic effect. This process occurs in semiconductor materials, such as silicon, within photovoltaic cells (solar cells). When photons from sunlight strike these cells, they excite electrons, generating a flow of direct current (DC) electricity. The Key Components of a PV System:

- Solar Panels (Modules): Arrays of interconnected PV cells that capture sunlight.
- Inverter: Converts DC electricity from the panels into alternating current (AC) for use in homes, businesses, or the grid.
- Mounting System: Structures to secure panels on rooftops, ground mounts, or tracking systems [27].

As illustrated in Figure (2.1), a photovoltaic system comprises four functional blocks. The first block is the energy source (solar panel), followed by a DC-DC static converter as the second block. The third block corresponds to the load, while the fourth represents the control system. The primary role of the DC-DC static converter is to perform impedance matching, ensuring the solar panel operates at its maximum power point (MPP) to deliver optimal energy output [28].

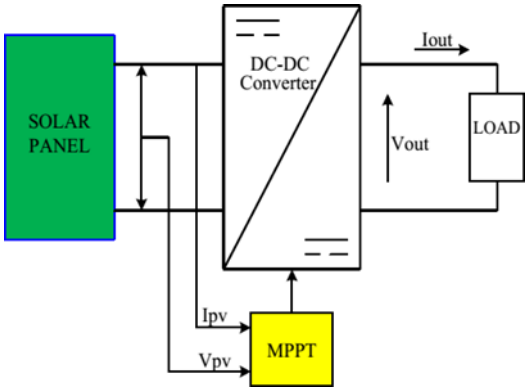

Figure 2.1 Photovoltaic system.

2.4 Functioning of photovoltaic system

Simply put, PV systems are like any other electrical power generating systems, just the equipment used is different than that used for conventional electromechanical generating systems. However, the principles of operation and interfacing with other electrical systems remain the same, and are guided by a well-established body of electrical codes and standards.

Although a PV array produces power when exposed to sunlight, a number of other components are required to properly conduct, control, convert, distribute, and store the energy produced by the array.

Depending on the functional and operational requirements of the system, the specific components required may include major components such as a DC-AC power inverter, battery bank, system and battery controller, auxiliary energy sources and sometimes the specified electrical load (appliances). In addition, an assortment of balance of system (BOS) hardware, including wiring, overcurrent, surge protection and disconnect devices, and other power processing equipment. Figure (2.2) show a basic diagram of a photovoltaic system and the relationship of individual components [29].

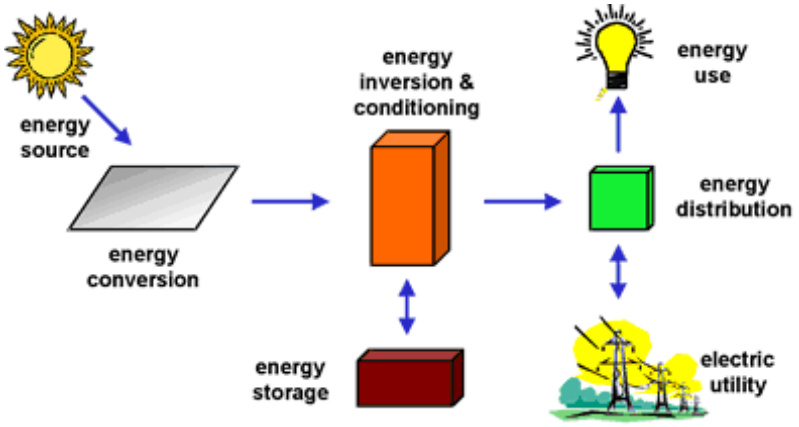

Figure 2.2 Major photovoltaic system components

2.5 The Different Types of Solar Photovoltaic Systems

There are three main types of solar PV systems: grid-tied, hybrid and off-grid. Each type of solar panel system has their advantages and disadvantages

2.5.1 On-Grid Solar System

An on-grid solar system or grid tied, is a solar PV system which connects directly to the National Grid. This kind of Solar PV System is the most common amongst home and business owners. This type of system is perfect for someone who is already connected to the Grid, yet wants to reduce their carbon footprint and energy bills.

An on-grid solar system doesn't require a battery storage system, and is connected to the National Grid directly via a Solar or micro inverter. As the solar panels convert sunlight into energy, your home uses this green energy supply to power your appliances. When you generate any excess solar energy, this electricity is exported back to the Grid.

A significant benefit of an on-grid solar PV system is the assurance of continuous energy supply through its connection to the National Grid. However, a notable drawback lies in its reliance on grid-tied inverters: if the National Grid experiences a failure, the solar system also shuts down, leaving users without backup power. This limitation, though, is not permanent. On-grid systems can be seamlessly upgraded to hybrid configurations by integrating a battery storage solution at any stage [30].

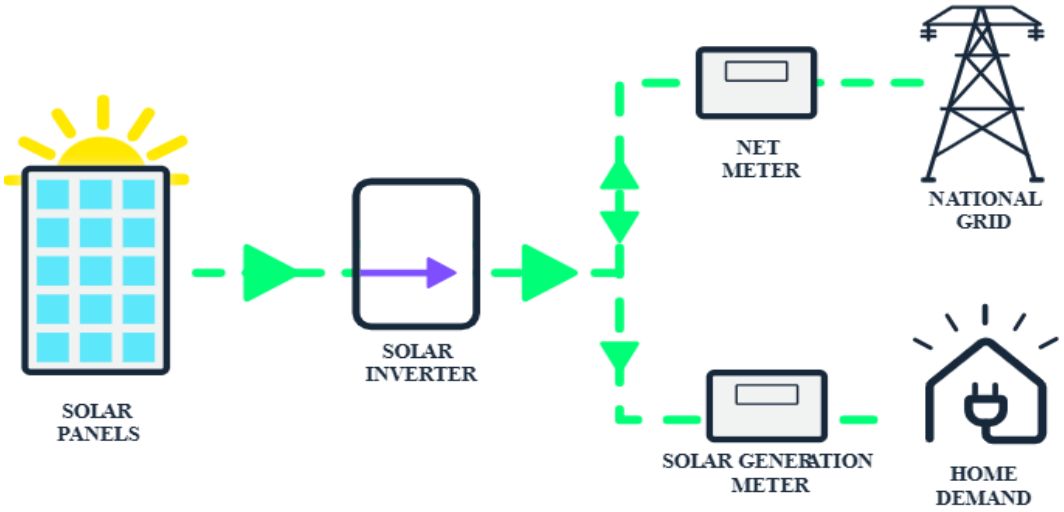

Figure 2.3 On-Grid Solar System

2.5.2 Hybrid Solar System

Hybrid Solar systems combine the technology of Solar Panels and Solar batteries to create a green energy solution which provides a back-up supply of energy. Although a hybrid PV system remains connected to the National Grid, any solar energy generated is first stored in a home battery solution before going to the grid.

A hybrid solar system's primary benefit lies in its ability to store surplus solar energy in batteries, enabling households to utilize solar power overnight while minimizing energy fed back into the grid. Additionally, unlike purely grid-tied systems, hybrid setups allow users to access stored battery power during grid failures a feature termed islanding making them ideal for regions prone to frequent power outages. Hybrid systems excel in flexibility: even when battery reserves are depleted, the grid remains a reliable backup source. This dual functionality positions hybrid solar as a balanced solution, bridging the gap between cost-effective on-grid systems and self-sufficient off-grid setups. While hybrid systems are more affordable than off-grid configurations, they incur higher costs than basic grid-tied systems [31].

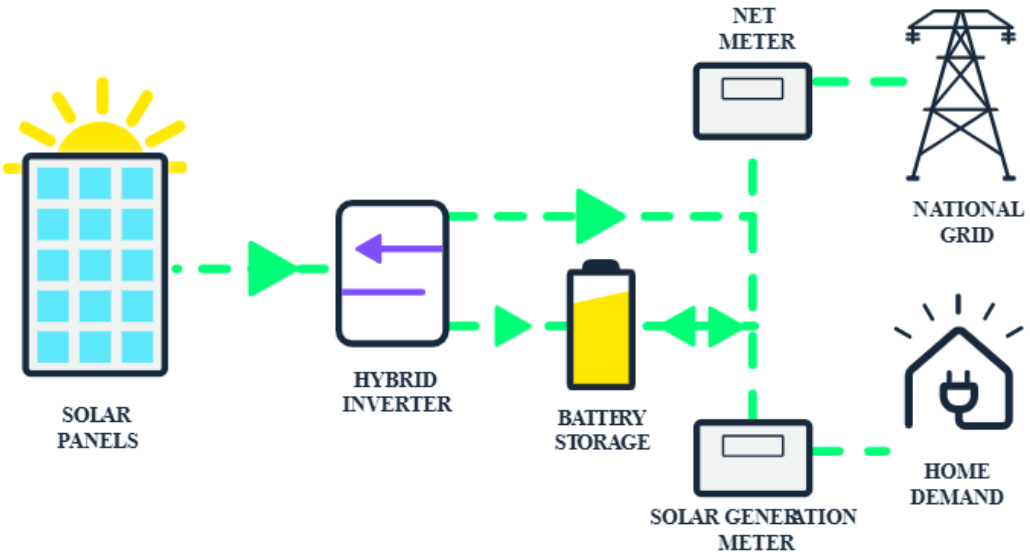

Figure 2.4 Hybrid Solar System

2.5.3 Off-Grid Solar System

PV systems can be installed without being connected with the conventional grid lines are off grid system. Off-grid solar PV system can be less expensive than expanding electrical cables in certain far-off regions. Another enormous preferred position of going off network is that, 100% autonomy from the power retailers. Need not to pay anything for the power costs, and 100% guaranteed against rising vitality measure. This system protects from grid-tied power failures or blackouts [30].

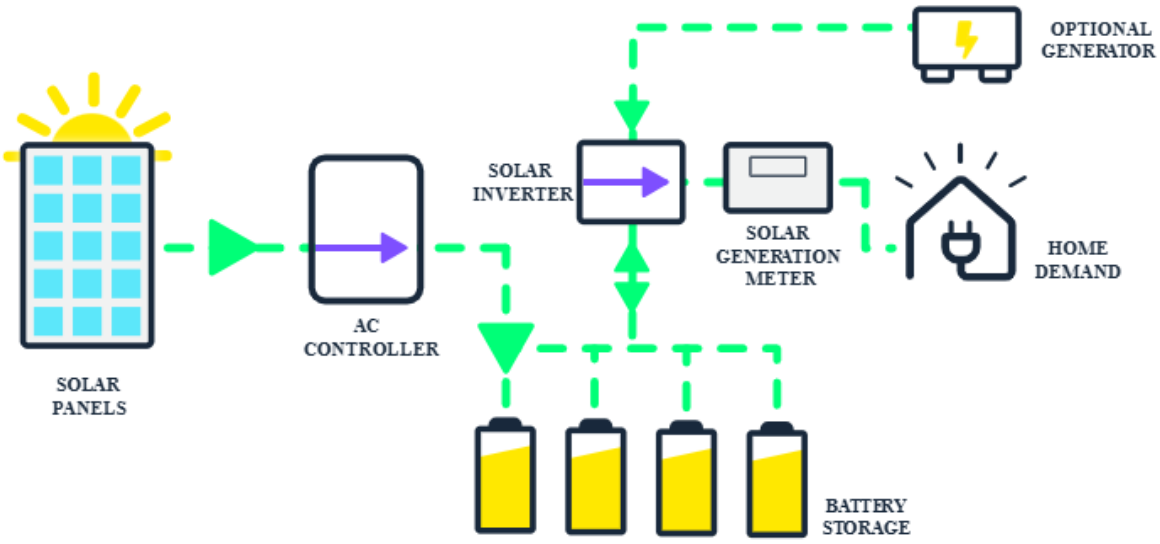

Figure 2.5 Off-Grid Solar System

2.6 Modeling of the photovoltaic system

A photovoltaic (PV) system can be tailored to meet specific electrical characteristics such as power, current, and voltage by arranging interconnected PV cells in series, parallel, or hybrid configurations. These cells, structured as the fundamental building blocks of a PV module, enable precise control over the system's output performance through their combined electrical properties [32].

2.6.1 Photovoltaic Cell Model

The basic electrical model of a photovoltaic (PV) cell used in this research comprises a current source connected in parallel with an ideal diode, as illustrated in Figure 2.6. This simplified equivalent circuit captures the photovoltaic effect, with the current source producing a light-generated current that scales with incident solar radiation. The diode represents the characteristic behavior of the semiconductor junction. For improved accuracy, more sophisticated models may include two parallel diodes to better replicate the cell's nonlinear electrical properties [33]. Additionally, two resistors are included:

- Series resistance (Rs): Represents resistive losses in the cell's material and contacts.
- Shunt resistance (Rp**)**: Models leakage currents due to imperfections in the semiconductor junction [34].

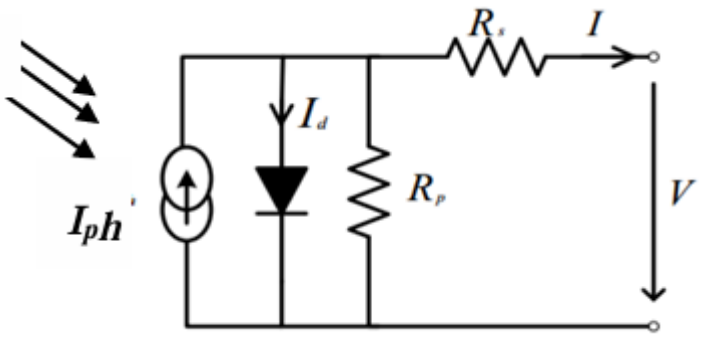

Figure 2.6 Equivalent circuit of a solar cell.

By applying the Kirchhoff Rule:

$$Ig=Id+Ip+I \tag{2.1}$$

The equation of the diode current:

$$I_d = I_0 \left(exp\left(\frac{V+R_S.I}{v_t.a}\right) - 1\right) \tag{2.2}$$

The current is given in resistance parallel:

$$I_p = \frac{V+R_S.I}{R_p} \tag{2.3}$$

From (2.1) we get current expression as:

$$I = I_g - I_d - I_p \tag{2.4}$$

The nonlinear equation describes how a PV Cell's characteristic (I-V) functions.

$$I = I_g - \left(I_0 \left(\exp\left(\frac{V+R_S.I}{v_t.a}\right) - 1\right)\right) - \frac{V+R_S.I}{R_p} \tag{2.5}$$

Where:

- Rs: The resistance series cell [Ω]
- *R*p: is the parallel resistance
- I_0: Saturation current (A)
- K is the Boltzmann constant; I and V are the terminal current and voltage of the PV cell
- V_t: the thermal voltage of the module: Vt=Ns kT/q, with Ns the number of cells connected in series
- q: electron's charge e = 1.6 *10^{-19} C

As depicted in Figure 2.7, the photovoltaic (PV) cell exhibits a nonlinear output characteristic, which shifts dynamically in response to meteorological conditions such as irradiance and temperature. Due to the significant variation in the optimal power point under changing environmental factors, the power converter's switching mechanism must be regulated by a dedicated algorithm to ensure accurate maximum power point tracking (MPPT) [35].

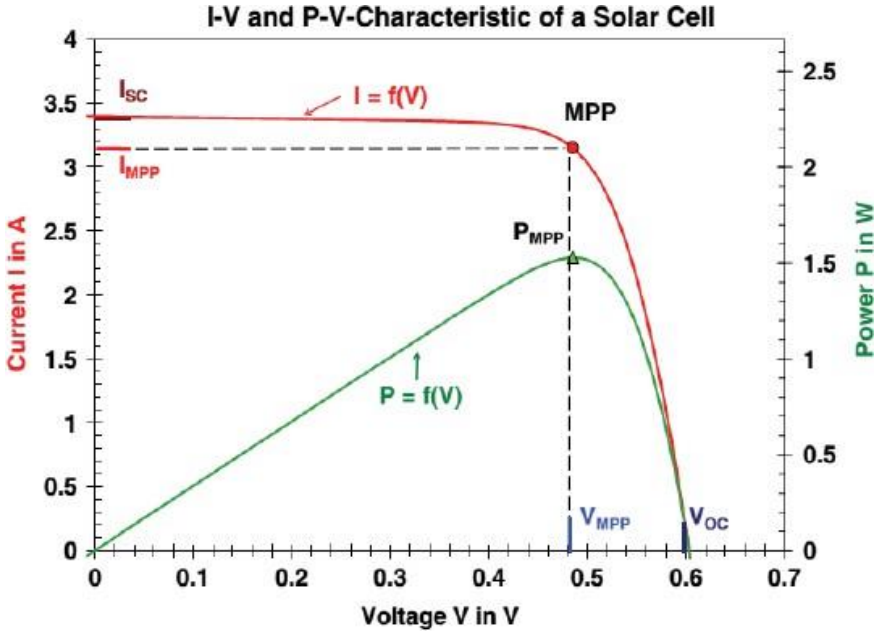

Figure 2.7 I-V and P-V characteristics of a photovoltaic cell

2.7 Maximum Power Point Tracking (MPPT) Controllers.

To address the dynamic operating points inherent in photovoltaic (PV) systems, specialized control strategies collectively termed Maximum Power Point Tracking (MPPT**)** are employed. The core objective of MPPT algorithms is to locate and maintain the maximum power point (MPP) by dynamically optimizing the impedance match between the PV generator and the load, ensuring maximum power transfer efficiency. This is achieved by automatically adjusting the duty cycle of the power converter's switching mechanism, which forces the system's operating point to remain at its optimal value despite weather fluctuations (e.g., irradiance/temperature changes) or abrupt load variations [36]. For this reason, three widely used MPPT control technique will be analyzed.

2.7.1 Perturb and Observe (P&O) controller

The Perturb and Observe (P&O) algorithm is widely adopted in practical applications, primarily owing to its straightforward implementation and simplicity. True to its name, the method operates by introducing a perturbation either increasing or decreasing the reference voltage which directly adjusts the duty cycle of the DC-DC converter. Following this adjustment, the algorithm observes the resulting change in the solar panel's output power. If the current power value P(k) exceeds the previous measurement P(k−1), the perturbation direction (e.g., increasing or decreasing in V ref) is maintained. Conversely, if the power decreases, the

perturbation direction is reversed in the next cycle. This iterative process ensures continuous optimization toward the maximum power point (MPP). The workflow of the P&O algorithm is summarized in the flowchart shown in Figure 2.8

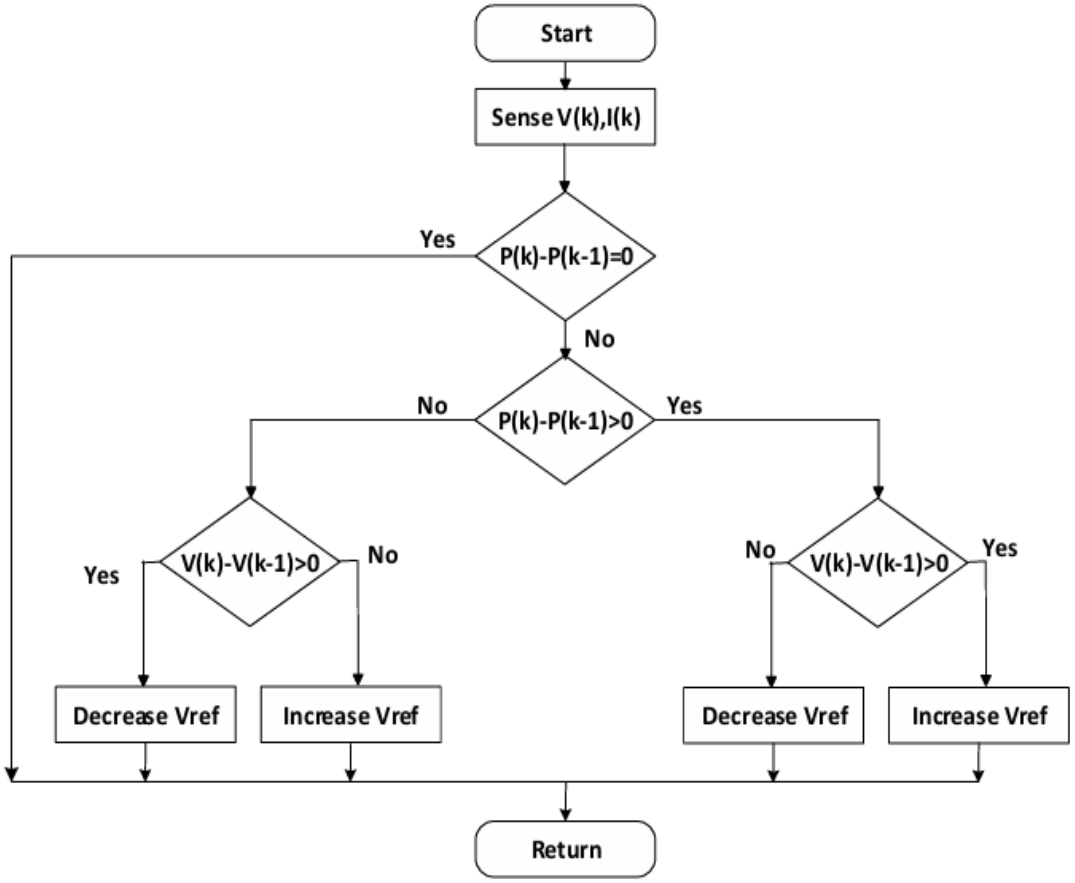

Figure 2.8 Flowchart Perturb and Observe Algorithm

2.7.2 Incremental Conductance (INC) Controller

Figure 5 presents the operational flowchart of the Incremental Conductance (INC) algorithm. The algorithm determines the operating point's position relative to the maximum power point (MPP) by analyzing the system's instantaneous conductance (I/V) and incremental conductance (dI/dV). The MPP is tracked through a comparison of these two parameters: if the instantaneous conductance (I/V) exceeds the negative incremental conductance (dI/dV), the duty cycle (d) is increased to shift the operating point toward the MPP. Conversely, if the condition is not met, the duty cycle is reduced to optimize power extraction [35]. This decision-making process enables the algorithm to dynamically adjust the system's operating conditions, ensuring stable convergence at the MPP under varying environmental or load scenarios.

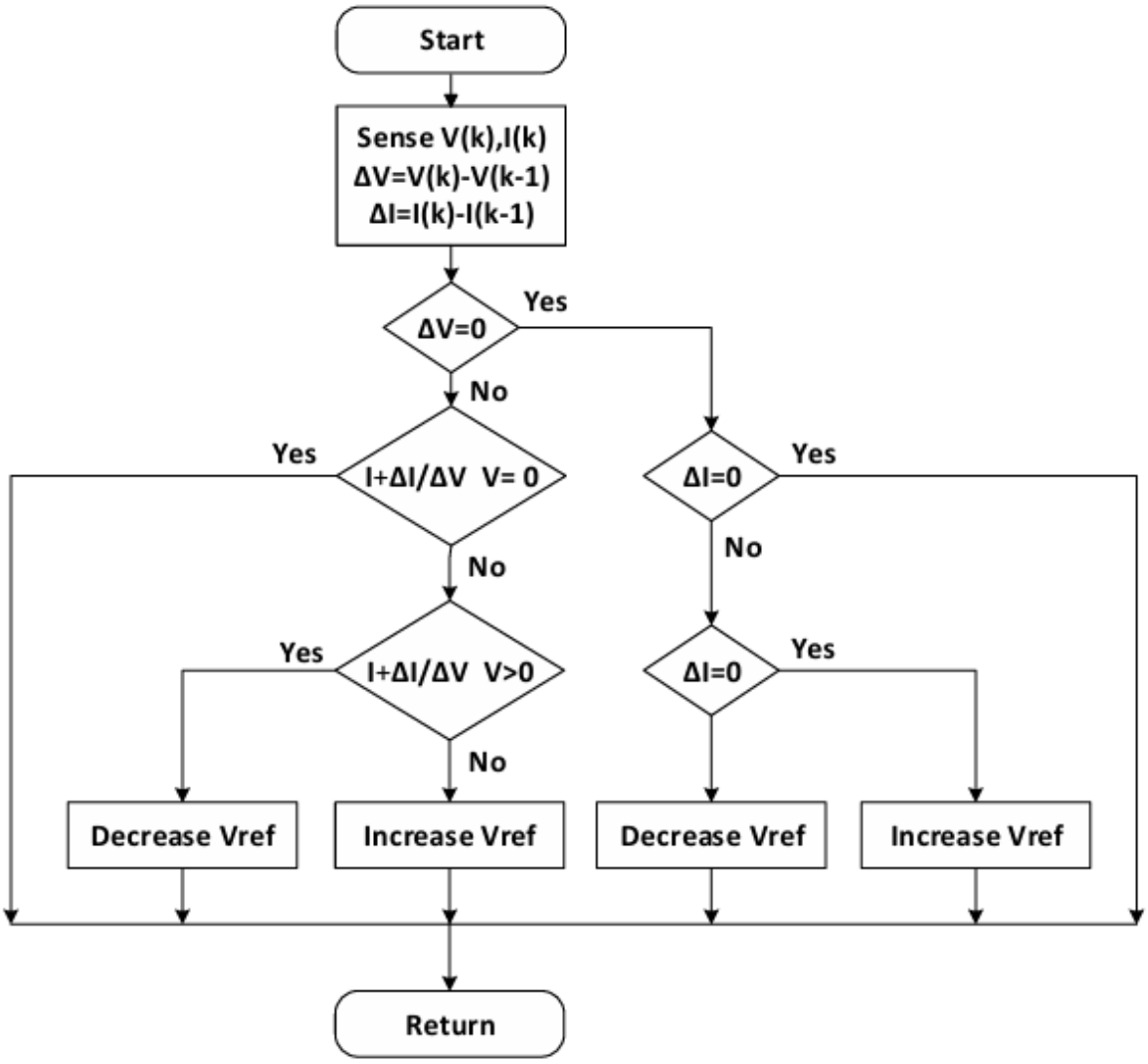

Figure 2.9 Flow Chart of INC Algorithm

2.7.3 Fuzzy logic controller (FLC)

Fuzzy logic control (FLC) is the most active research area in the application of fuzzy set theory, fuzzy reasoning, and fuzzy logic. The application of FLC extends from industrial process control to biomedical instrumentation and securities. Compared to conventional control techniques, FLC has been best utilized in complex ill-defined problems, which can be controlled by an efficient human operator without knowledge of their underlying dynamics [37]. The structure of a process controlled via a fuzzy controller is shown in Figure 6, which emphasizes the basic components of a fuzzy controller: Fuzzification, Fuzzy Rule base and Interfacing engine and Defuzzification (fuzzy refer).

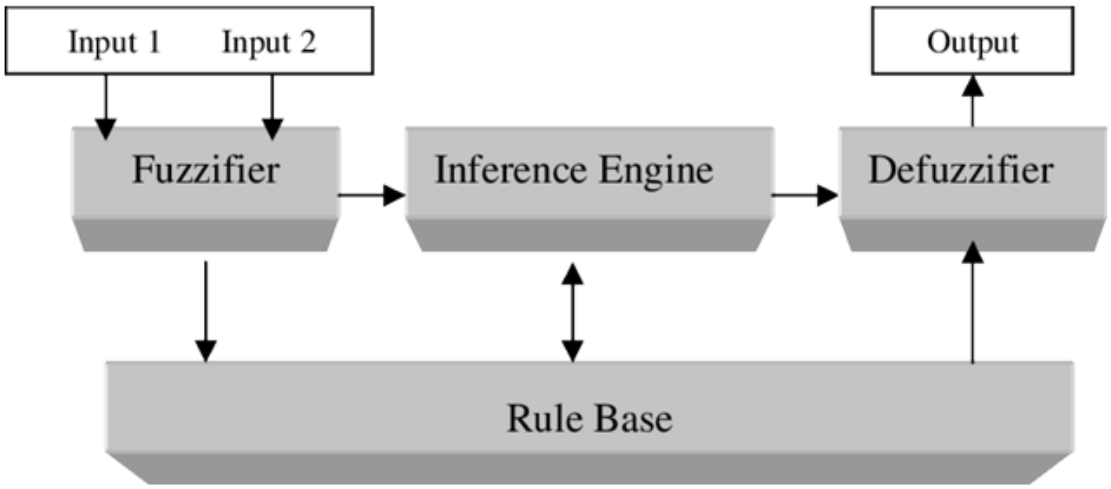

Figure 2.10 the basic components of a fuzzy controller

- **Fuzzification:** The fuzzification allows conversion of physical variables of entry into fuzzy sets [38]. In our case, we have two inputs the error E and the variation in the error ΔE defined as follows:

$$E(n) = \frac{P(n)-P(n-1)}{V(n)-V(n-1)} \tag{2.6}$$

$$\Delta E(n) = E(n) - E(n-1) \tag{2.7}$$

- **Inference method:** The inference engine determines the fuzzy output by applying a rule to the fuzzy input. To get a suitable linguistic value, the rule must first be assessed after the actual input value has been fuzzified. By introducing the least amount of disturbance to the solar voltage output, it is possible to identify the quick variations in PV power consumption. [39].
- **Defuzzification:** is the technique of using two algorithms the center of area (COA) and the maximum criterion method (MCM) to extract a single number from the output. [39].

2.8 Conclusion

Photovoltaic energy is a clean, accessible, abundant, and inexhaustible form of energy that offers exciting development prospects. In many countries, the solar photovoltaic sector is expanding rapidly, thanks in particular to the connection of equipment to the national grid and incentives for users and industries to exploit it.

Chapter III:

Results and Discussion

chapter 3: Results and Discussion

3.1 Introduction

To confirm the control strategy (SBC) and the open-loop and closed-loop splitting of the Z-Source inverter, simulations were conducted on MATLAB (Simulink).

3.2 Simulation of Open-Loop Control for Z-Source Inverter (SBC Method):

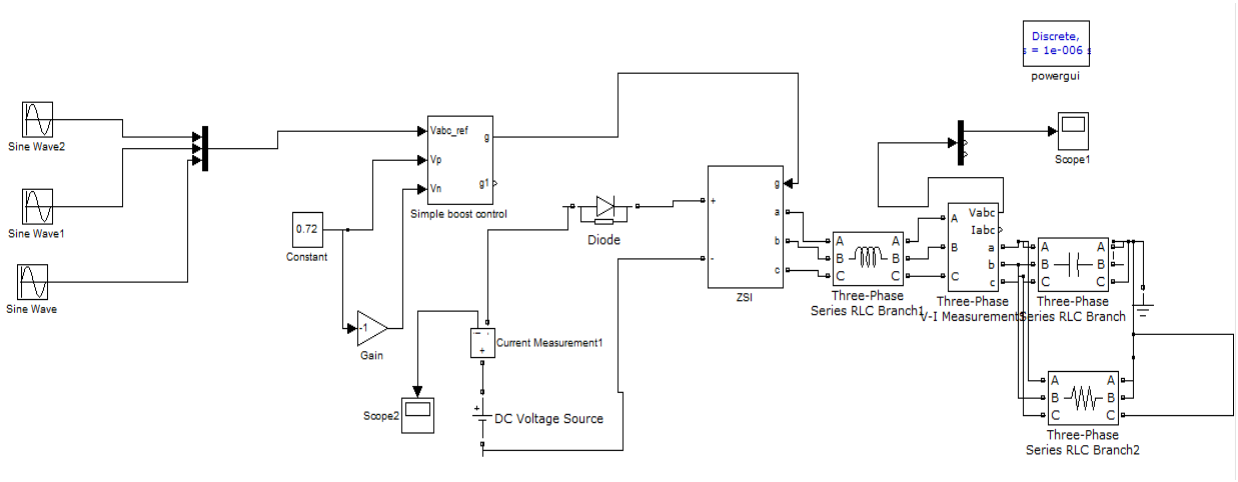

Figure 3.1: Open-Loop Control for Z-Source Inverter

Figure 3.1 shows a hardware model of a three-phase open-loop inverter with the following parameters:

Table 3-1: System Parameters for open-loop

parameters	values
DC input voltage of the inverter	Vdc = 300(V)
ZS inductances	L1=L2=L = 10e-3 (H)
ZS capacitances	C1=C2=C= 4700e-6 (F)
Filter parameters	Lf = 10e-3(H), Rf = 10 (Ω), Cf=300e-6(F)
Nominal frequency	F = 50 (Hz)
Switching frequency	fs= 5000 (Hz)
Sampling time	Ts = 1e-006 (s)

3.2.1 Results of simulation

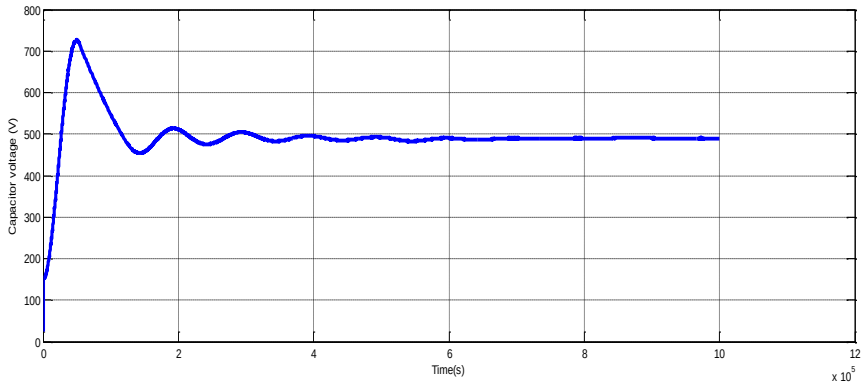

Figure 3.2: capacitor voltage of ZSI

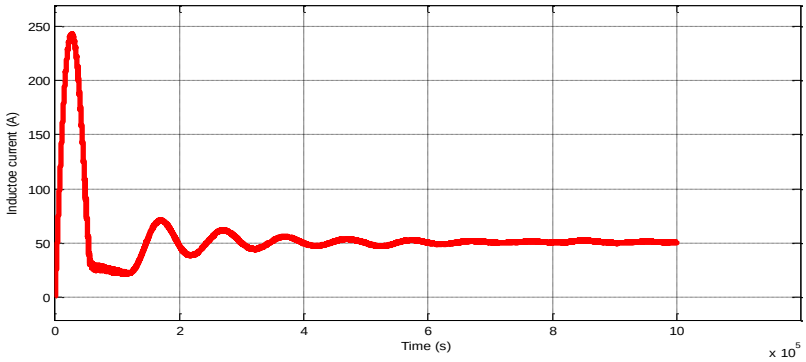

Figure 3.3: Inductor current of ZSI

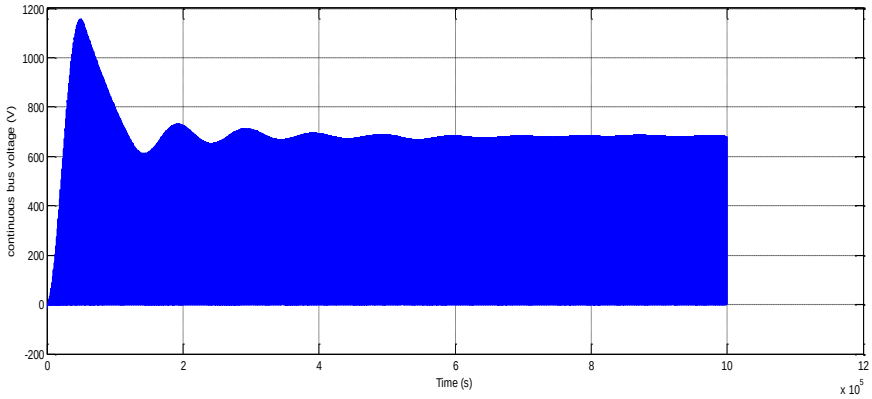

Figure 3.4: continues bus voltage

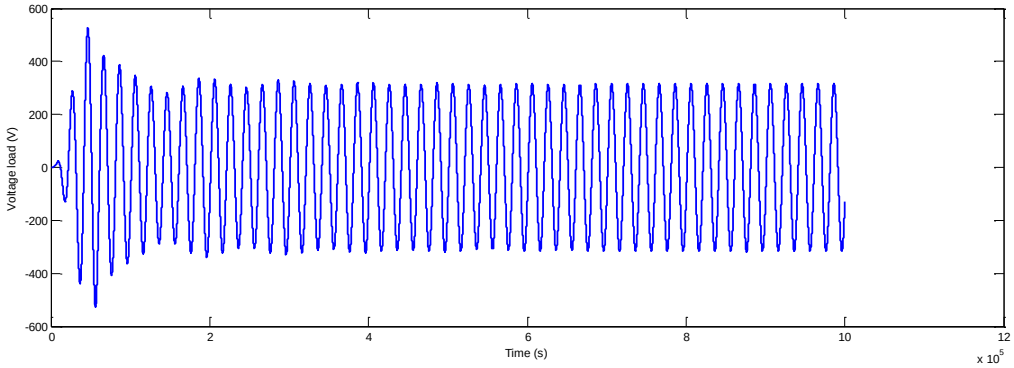

Figure 3.5: voltage load

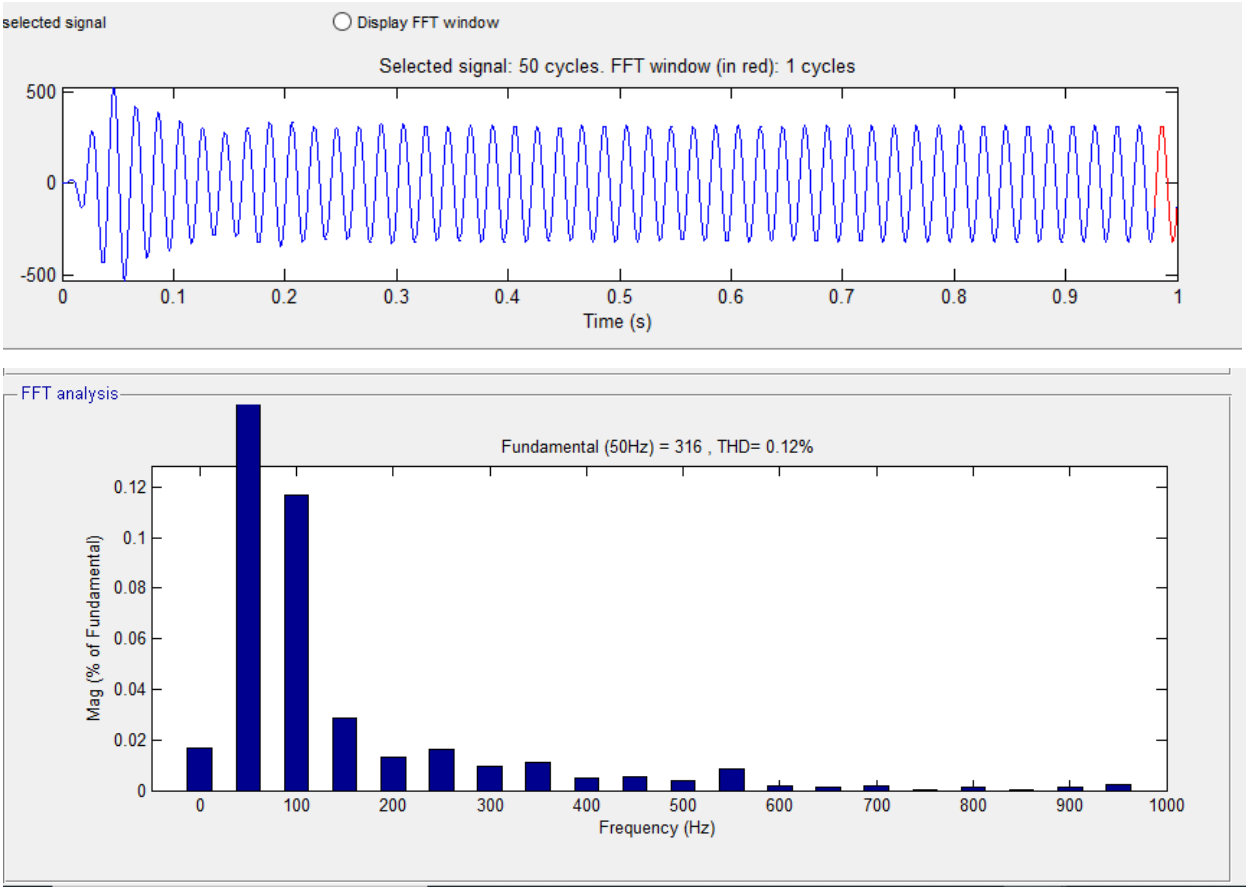

Figure 3.6: Fundamental components and total harmonic distortion (THD)

3.2.2 Interpretation of results:

The simulation results of the open-loop control strategy based on the Shoot-Through Boost Control (SBC) method for the Z-Source Inverter (ZSI) validate the effectiveness of the proposed approach in achieving stable voltage regulation and acceptable harmonic performance. As illustrated in Figure 3.2, the capacitor voltage (VCZ) rises quickly and stabilizes around 490 V, demonstrating the inverter's capability to boost the input voltage of 300 V efficiently. Figure 3.3 shows that the inductor current (ILZ) responds dynamically to changes in load, indicating appropriate current adaptation within the system. The inverter's input voltage, depicted in Figure 3.4, confirms successful voltage amplification through the ZSI structure, governed by the boost factor (B). Additionally, the filtered AC output voltage presented in Figure 3.5 reaches a stable value of approximately 316 V, reflecting effective voltage conversion and filtering. Spectral analysis results shown in Figure 3.6 reveal a low Total Harmonic Distortion (THD), which confirms the system's ability to produce high-quality AC output. These results collectively affirm the viability of the SBC open-loop control strategy for ZSI configurations in power electronic applications requiring voltage boosting and low harmonic distortion.

3.3 Simulation of Closed-loop Control for Z-Source Inverter (SBC Method):

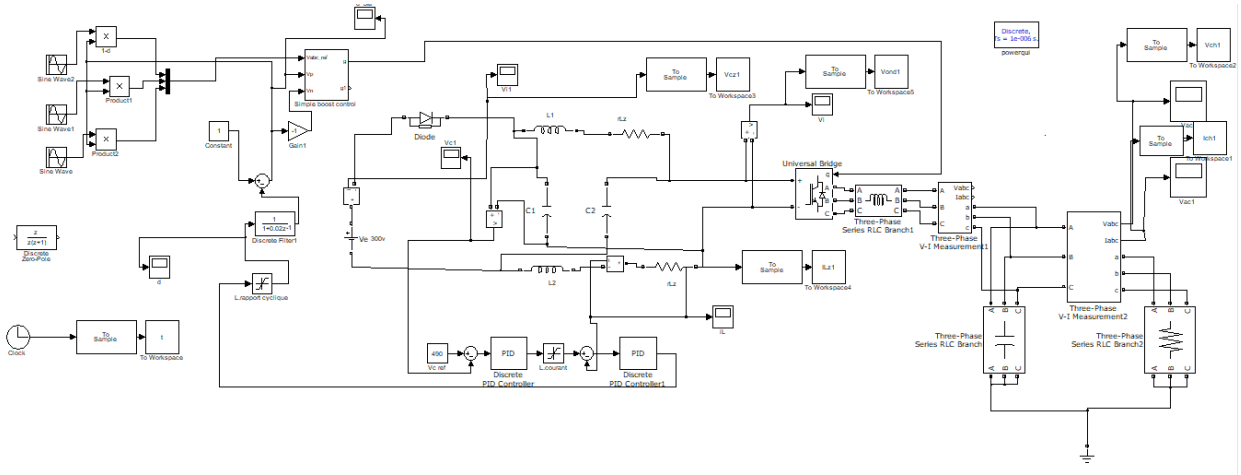

Figure 3.7:close-Loop Control for Z-Source Inverter

Figure 3.7 shows a hardware model of a three-phase closed-loop inverter with the following parameters:

Table 3-2: System Parameters for closed-loop

parameters	Values
DC input voltage of the inverter	Vdc = 300(V)
ZS inductances	L1=L2=L = 10e-3 (H)
ZS capacitances	C1=C2=C= 480 (F)
ZS Resistance	Rz=0.01(ohms)
Nominal frequency	F = 50 (Hz)
Switching frequency	fs=5000 (Hz)
Sampling time	Ts = 1e-006 (s)

3.3.1 Results of Simulation:

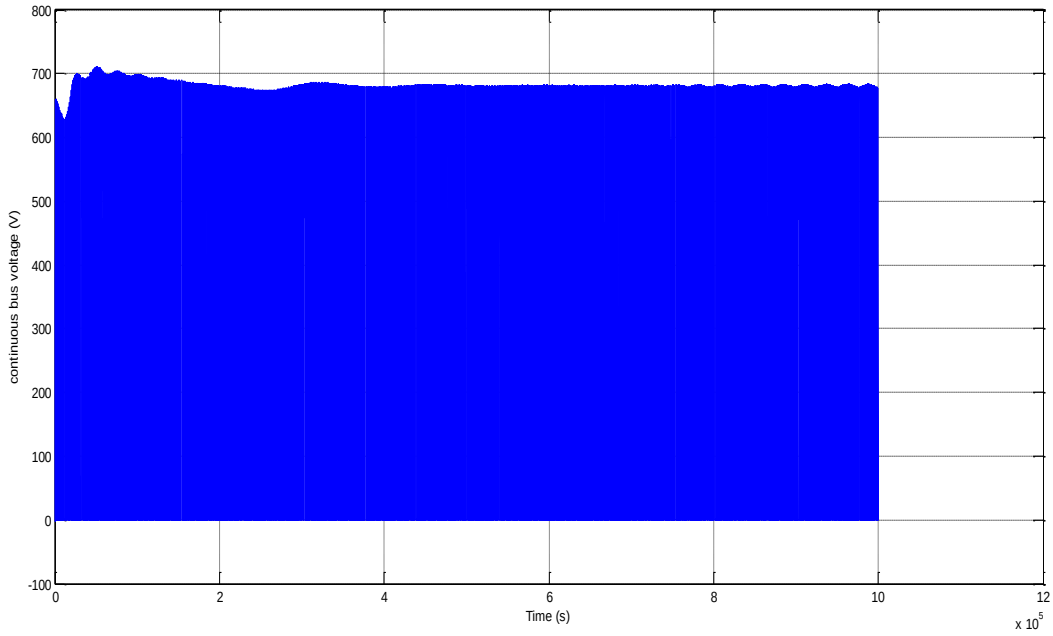

Figure 3.8: input voltage of the inverter Vi

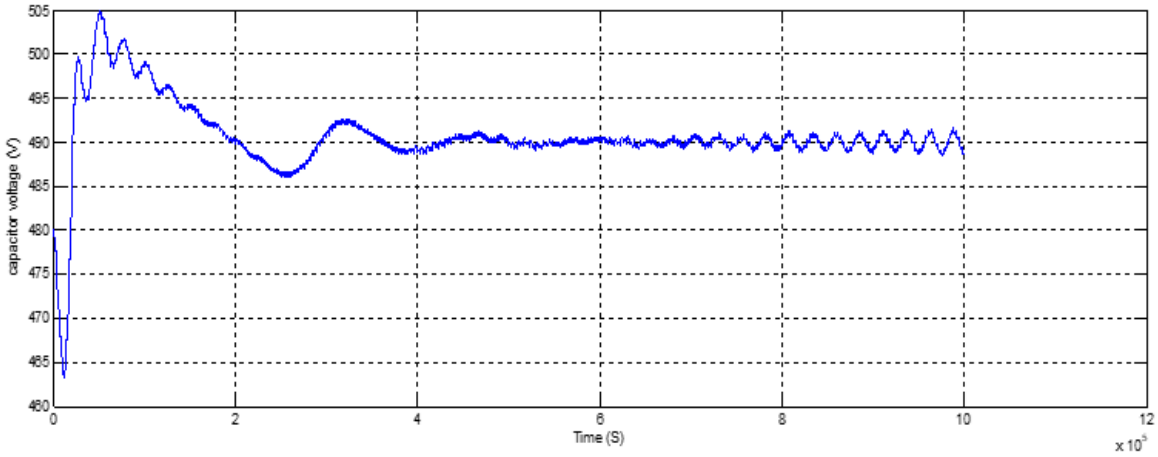

Figure 3.9:voltage across the capacitors VCz

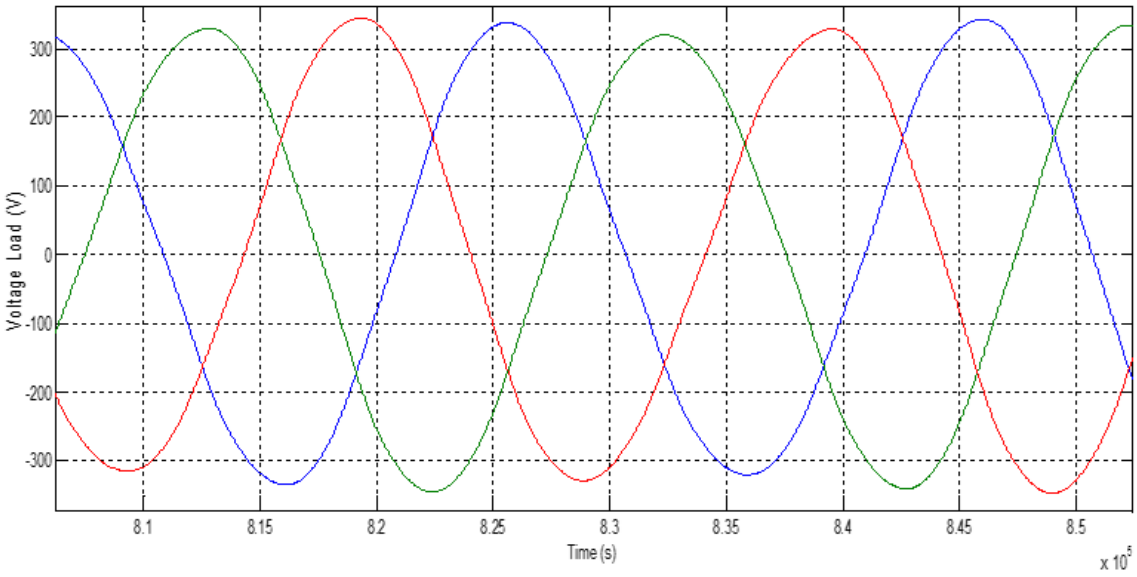

Figure 3.10:simple filtered three-phase load voltage

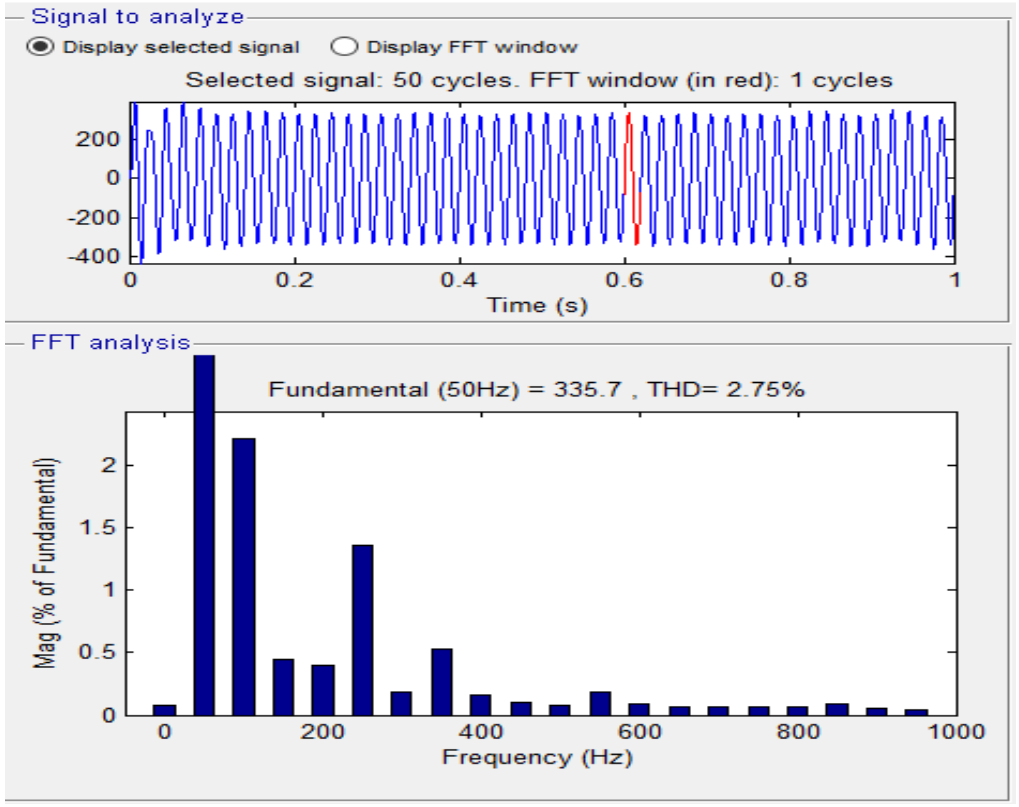

Figure 3.11: Fundamental components and total harmonic distortion (THD)

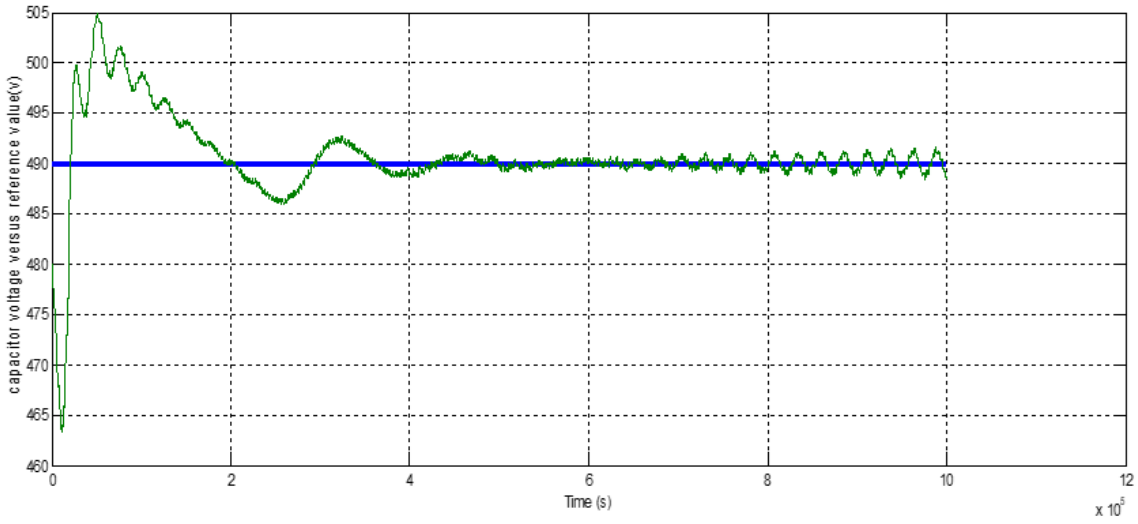

Figure 3.12:voltage across capacitor VCz compared with the reference value

3.3.2 Interpretation of results:

The simulation results of the closed-loop control for the Z-Source Inverter (ZSI) using the SBC (Simplified Boost Control) method highlight the system's effective performance under predefined electrical parameters. With a DC input voltage of 300 V, equal inductances of 10 mH, and capacitors rated at 480 µF, the inverter operates at a nominal frequency of 50 Hz and a high switching frequency of 5 kHz, as outlined in Table 32. The input voltage (Figure 3.8) and capacitor voltage (VCz) (Figure 3.9) demonstrate stable waveform characteristics, indicating robust voltage regulation. The filtered three-phase output voltage (Figure 3.10) exhibits minimal distortion, suggesting efficient output voltage synthesis. Notably, the Total Harmonic Distortion (THD) shown in Figure 3.11 confirms that the system achieves low harmonic content, a critical performance indicator for power quality. Additionally, the comparison of VCz with its reference value (Figure 3.12) validates the controller's ability to maintain capacitor voltage within desired limits. These results collectively demonstrate the efficacy of the closed-loop SBC method in enhancing inverter stability, minimizing harmonic distortion, and ensuring reliable power conversion in ZSI-based systems.

3.4 Conclusion

This chapter examines the control of the Z-source inverter (ZSI) by PI controller using a DC voltage source, with the aim of improving performance results.

The proposed Z-source inverter was found to be more efficient, higher performing, more economical and requiring fewer active components.

General Conclusion

This master's thesis focused on the integration of Z-source inverters (ZSI) into photovoltaic (PV) energy systems, which is a promising solution to enhance the performance and reliability of solar energy conversion. Unlike traditional voltage-source or current-source inverters, the Z-source inverter provides both buck and boost capabilities in a single-stage topology, which simplifies system design, improves robustness, and increases overall efficiency.

The main objective of this work was to design and control a ZSI powered by a photovoltaic panel using the Simple Boost Control (SBC) strategy. The system was modeled and simulated using MATLAB/Simulink, allowing for a detailed analysis of its behavior under different operating conditions.

In addition, the use of a PI (Proportional-Integral) controller helped ensure stable system performance, with fast response times to input changes and good resistance to disturbances. The simulation results demonstrated that the proposed system architecture can effectively reduce input current ripple, minimize stress on switching devices, and maintain a high-quality output voltage.

This study confirmed that integrating a ZSI with appropriate control strategies significantly enhances the energy conversion process in photovoltaic applications. It offers a promising alternative for standalone and grid-connected renewable energy systems, especially in regions with variable environmental conditions.

Future Perspectives

- Integration of the structure studied in the field of electric traction, with the use of nonlinear control methods.
- Minimization of sensors used for ZSI inverter control.

bibliographic references

1. Reisi, A. R., Moradi, M. H., & Jamasb, S. (2013). Classification and comparison of maximum power point tracking techniques for photovoltaic systems: A review. Renewable and Sustainable Energy Reviews, 19, 433–443.
2. Bhatnagar, P., & Nema, R. K. (2013). Maximum power point tracking control techniques: State-of-the-art in PV applications. *Renewable and Sustainable Energy Reviews*, 23, 224–241.
3. Shen, M., Joseph, A., Wang, J., Peng, F. Z., & Adams, D. J. (2005). Comparison of traditional inverters and Z-source inverter. *IEEE Transactions on Industry Applications*, 41(1), 254–262.
4. Peng, F. Z. (2003). Z-source inverter. *IEEE Transactions on Industry Applications*, 39(2), 504–510.
5. Tang, Y., Loh, P. C., Blaabjerg, F., & Wang, X. (2012). Highly reliable Z-source inverter for photovoltaic systems. *IEEE Transactions on Industrial Electronics*, 60(4), 1284–1294.
6. Ali, A., Khan, M. A., & Al-Sulaiman, F. A. (2020). An overview of Z-source inverters and their control strategies for renewable energy applications. *Energies*, 13(15), 3862.
7. F. Z. Peng, "Z-source inverter," IEEE Transactions on Industry Applications, vol. 39, no. 2, pp. 504-510, March-April 2003.
8. M. Shen and F. Z. Peng, "Operation modes and characteristics of the Z-source inverter with small inductance or low modulation index," IEEE Transactions on Industry Applications, vol. 43, no. 2, pp. 543-552, 2007.
9. J. Anderson and F. Z. Peng, "Four quasi-Z-Source inverters," IEEE Power Electronics Specialists Conference, pp. 2743-2749, 2008.
10. M. Abdelghani Benziada, “Comparative Study of Z-Source Converter Topologies,” Master’s Thesis, École Nationale Polytechnique, 2015.
11. mohamed tayeb boussabeur, integration of z-source inverter in electrical systems, lmd doctorate, university of echahid hamma lakhdar - el oued,2023
12. M. K. Nguyen, Y. C. Lim, and G. B. Cho, "Switched-inductor quasi-Z-source inverter," IEEE Transactions on Power Electronics, vol. 26, no. 11, pp. 3183-3191, 2011.

13. Y. Liu, B. Ge, H. Abu-Rub, and F. Z. Peng, "Control system design of battery-assisted quasi-Z-source inverter for grid-tie photovoltaic power generation," IEEE Transactions on Sustainable Energy, vol. 4, no. 1, pp. 94-103, 2013.

14. J. M. Carrasco, L. G. Franquelo, J. T. Bialasiewicz, and E. Galván, "Power-electronic systems for the grid integration of renewable energy sources: A survey," IEEE Transactions on Industrial Electronics, vol. 53, no. 4, pp. 1002-1016, 2006.

15. Tayeb, Boussabeur & Rabhi, Boualaga & Aboelsaud, Raef & Ibrahim, Ahmed & Toumi, Djaafar & Zellouma, Laid & Garganeev, Alexander. (2021). Current control of Z-source four-leg inverter for autonomous photovoltaic system based on model predictive control. 10.18799/24131830/2021/07/3280.

16. C. R. Gonzalez et al., "A New Perspective on Z-Source Inverter Topologies," Journal of Power Electronics Research, vol. 12, no. 3, pp. 213-221, 2017.

17. M. M. E. Jafar, S. H. T. K. Nabil, and S. S. Abdullah, "Control strategies for Z-source inverter: A review," IEEE Access, vol. 8, pp. 194145-194160, 2020.

18. S. Kim et al., "Robust Control for Z-Source Inverters in Industrial Applications," International Journal of Power Electronics, vol. 9, no. 2, pp. 145-152, 2018.

19. L. P. Martinez, "Cost Analysis of Z-Source Converters in Renewable Energy Systems," Renewable Energy Systems Journal, vol. 8, no. 1, pp. 65-73, 2016.

20. R. D. Johnson and P. Kumar, "Reduction of Harmonic Distortion in Z-Source Inverters Using Advanced Modulation Techniques," IEEE Transactions on Power Electronics, vol. 34, no. 4, pp. 3010-3018, 2019.

21. Ramkrishna Mishan, Xingang Fu, Chanakya Hingu, Poria Fajri, analyzing frequency spectrum and Total Harmonic Distortion for high switching frequency operation of GaN based filter-less multilevel cascaded H-bridge inverter, e-Prime - Advances in Electrical Engineering, Electronics and Energy, Volume 11,2025,100906, ISSN 2772-6711,

22. Bikash Gyawali, Aidha Muhammad Ajmal, Wenjie Liu, Yongheng Yang, A review on modulation techniques of Quasi-Z-source inverter for grid-connected photovoltaic systems-Prime - Advances in Electrical Engineering, Electronics and Energy, Volume 10,2024,100809, ISSN 2772-6711.

23. Jingbo Liu, Jiangang Hu, and Longya Xu,Dynamic Modeling and Analysis of Z Source Converter Derivation of AC Small Signal Model and Design-Oriented Analysis, IEEE IEEE Transactions on power electronics, VOL. 22, NO. 5, pp.1786,1796, SEPTEMBER 2007

24. Chaib, Ibtissam & Behlouli, Asma & Hadjaidji, Fatma & Ouarda, Benkouider & Berkouk, El Madjid. (2017). Comparative study between different control strategy of the z-source inverter. 1-6. 10.1109/ICEE-B.2017.8192064.

25. Mohamed, D.Hicham, theoretical study on perovskite solar cells (Pscs) and their applications, Thesis of master's degree, University of Kasdi Merbah Ouargla,2022.

26. Li, Qian & Zhang, Liming & Chen, Zhongwei & Quan, Zewei. (2019). Metal Halide Perovskites under Compression. Journal of Materials Chemistry A. 7. 10.1039/C9TA04930D.

27. (Https://www2.nrel.gov/research/re-photovoltaics) consulté le 15/02/2025

28. Rashid, M. H. (2018). Power Electronics Handbook: Devices, Circuits, and Applications (4th ed.). Butterworth-Heinemann.

29. https://www.fsec.ucf.edu/en/consumer/solar_electricity/basics/how_pv_system_works.htm consulté le 15/02/2025

30. (Https://www.deegesolar.co.uk/different_types_of_solar_pv_systems/) consulté le 17/02/2025

31. (Https://resources.system-analysis.cadence.com/blog/msa2021-the-different-types-of-solar-photovoltaic-systems) consulté le 20/02/2025

32. Aicha, D. & Teta, Ali & Rezaoui, Mohamed. (2018). Analysis of MPPT Methods: P & O, INC and Fuzzy Logic (FLC) for a PV System. 10.1109/CEIT.2018.8751820.

33. B. Omar, C. Idris, L'intégration du photovoltaïque Au Réseau Électrique Problèmes et perspectives, Mémoire d'ingénieur. Université de Biskra, 2006.

34. Bun, L. Détection et Localisation de Défauts pour un Système PV, Thèse de Doctorat en Génie Electrique, Université de Grenoble, 2011.

35. Harsha P.P., Dhanya P.M, Karthika K, "Simulation & Proposed Hardware Implementation of MP controller for a Solar PV system", International Journal of Advanced Electrical and Electronics Engineering, (IJAEEE) Volume-2, Isue-3, 2013

36. N. Drir, L. Barazane and M. Loudini, Fuzzy logic for tracking maximum power point of photovoltaic generator, Revue des Energies Renouvelables Vol. 16 N°1 (2013) 1 – 9

37. (Https://www.geeksforgeeks.org/fuzzy-logic-control-system/) consulté le 05/03/2025

38. Mr. OUARI Mondher et Mr. ZINE Yakoub, Étude des commandes MPPT d'un système Photovoltaïque, Mémoire de Projet de fin d'études, École nationale Polytechnique,2020.

39. Partha P. Biswas, P.N. Suganthan, Guohua Wu, Gehan A.J. Amaratunga, Parameter estimation of solar cells using datasheet information with the application of an adaptive

differential evolution algorithm, Renewable Energy, Volume 132,2019, Pages 425-438, ISSN 0960-1481, https://doi.org/10.1016/j.renene.2018.07.152.